The Role of ADAR1 in Innate Immune Regulation and Cell Biology

Kathleen M. Pestal

A dissertation
submitted in partial fulfillment of the
requirements for the degree of

Doctor of Philosophy

University of Washington

2016

Reading Committee:
Daniel B. Stetson, Chair
Michael Gale, Jr.
Savan Ram

Program Authorized to Offer Degree:
Department of Immunology

University of Washington

Abstract

The Role of ADAR1 in Innate Immune Regulation and Cell Biology

Kathleen M. Pestal

Chair of Supervisory Committee:
Associate Professor Daniel B. Stetson
Department of Immunology

Mutations in *ADAR*, which encodes the ADAR1 RNA editing enzyme, cause Aicardi–Goutières syndrome (AGS), a severe inflammatory disease associated with an aberrant type I interferon response. Aicardi–Goutières syndrome has previously been shown to result from ineffectual negative regulation of the cytosolic DNA sensing pathway. Here, we demonstrate that ADAR1 is a specific and essential negative regulator of the MDA5-MAVS RNA sensing pathway. Moreover, we uncovered an MDA5-MAVS-independent function for ADAR1 in the development of multiple organs, including the kidney and intestines. We also discovered a cell-intrinsic role for ADAR1 in B cell development. We showed that the p150 isoform of ADAR1 exclusively regulated the MDA5 pathway, whereas both the p150 and p110 isoforms contributed to development. Abrupt deletion of ADAR1 in adult mice revealed that both of these functions were required throughout life. Our findings define genetically distinct roles for both ADAR1 isoforms *in vivo*, with implications for the human diseases caused by *ADAR* mutations.

Table of Contents

Acknowledgements

"If I have seen further, it is by standing on the shoulders of giants."

Sir Isaac Newton

There are so many people who have helped me on this journey and to all I am extremely indebted for their time, patience and guidance. I thank my parents for showing me what dedication, hard work, responsibility and generosity looks like. I wouldn't be here in any capacity without them. I thank my oldest BFFs, Karly and Malia, and my newest BFF, April, for keeping me grounded and sane, as best they can from a distance. Thank you for knowing me and still liking me. Thank you to Nataliya, Heiyoun, Benjamin, Stephanie, their families and the rest of the Berkeley/Raulet crew for their love and their tireless efforts to get me here and to keep me going. I thank the Stetson Lab and the many UW Immunology trainees for the inside jokes and camaraderie which have lightened the load. I thank my committee and the entire UW Immunology faculty and staff for their continued support and wisdom.

I have stood on the shoulders of two scientific giants in my pursuit of this doctorate: Dr. David Raulet and Dr. Dan Stetson. Dr. Raulet took me from an amorphous lump of clay and fashioned me, in his image, into something that kinda-sorta looked like a scientist. I can never thank him enough for willingly giving me his time and expertise. I can only hope to pay it all forward. It is under the guidance of Dr. Dan Stetson that I have polished some of the remaining edges. Thank you for being the positive to my negative, the Yin to my Yang. Your steadfast optimism and dedication to me and my project helped weather the many storms. Thank you for appreciating the little things about science that we both love and for being on my side when it has mattered most. I am a better scientist and person for having been here.

Chapter 1: Introduction

Innate Immunity to Viral Infection

The ability to distinguish between self and non-self is a fundamental characteristic of immune recognition and is achieved through a variety of mechanisms ranging from very broad to extremely specific. The immune system is divided into two parts: the innate and the adaptive components. The adaptive immune response (effects carried out by antibodies, B cells and T cells) is the more familiar of the two and is characterized by its nearly unlimited specificities and long-term, antigen-specific responses known as "immunologic memory". Understanding the function and mechanism of adaptive immunity was the primary focus of immunological research for nearly 70 years. It was known, but largely ignored through the majority of the twentieth century, that there were immune functions outside of the adaptive response. This changed in the late 1980s with the proper emergence of the field we now know as innate immunology (1-3).

The features of innate immunity are distinguished from adaptive immunology as being mediated by germline-encoded receptors and performed, to some extent, by all cell types in all organisms. Due to the conserved nature of these receptors, they target essential features of microbes that are not found in the host. This allows for a simple way to determine self versus non-self and targeting indispensable molecules ensures the encoded receptors retain function in the presence of evolutionary pressure. For receptors that target cellular organisms, features of the cell membrane are often targeted, as they are essential and difficult for the pathogen to change. In contrast, the host produces all of the viral components, making self/non-self discrimination very difficult. The only invariant feature all viruses share is that they contain a nucleic acid genome. Given that viral pathogens infect all cellular life, nucleic acid recognition as an anti-viral defense is conserved in all organisms. In Bacteria and Archaea, these mechanisms include antisense RNA, restriction enzymes and CRISPR-Cas9. Eukaryotes have retained many

of these same mechanisms (Fig 1.1), but increasing cellular complexity also resulted in increased diversity of anti-viral defenses (4).

Cell-intrinsic detection of nucleic acids is necessary for proper defense against viral infection (5). Cyclic GMP-AMP synthase (cGAS) (6) binds double-stranded DNA in the cytosol and produces the secondary messanger molecule cGAMP. This cyclic dinucleotide then binds to and activates the signaling adapter STING (*TMEM173)* (5),(7). Similarly, cytosolic RNAs, like those from RNA viral genomes, are sensed by either of the members of the DExD/H-box helicase family known as the RIG-I-like Receptors (RLRs): RIG-I (*DDX58*) or MDA5 (*IFIH1*) (8, 9). RNA is bound by the helicase domain of the RLR and the CARD domain allows the interaction with the signaling adapter MAVS (Mitochondrial Anti-Viral Signaling protein, aka VISA/IPS-1/CARDIF) (10). The activation of a variety of molecules occurs downstream of both of these pathways leading to the activation of the transcription factors IRF3 and NFκB. The nuclear localization of these transcription factors induces the expression of many inflammatory cytokines, including TNFα, IL-6 and type I interferons, as well as a host of other anti-viral molecules known as the interferon-stimulatory genes. The increased expression pattern of the gene is known as an "interferon signature" and is a hallmark of viral infection (11).

Regulation of Cytosolic Sensing

Unrestrained or constitutive immune responses can lead to cellular death and tissue damage. Like all elements of the immune response, it is important that the cell-intrinsic nucleic acid sensing pathways are carefully regulated to prevent aberrant signaling and autoimmunity. There are several mechanisms by which the host regulates these pathways and self/nonself discrimination occurs through all of them to varying degrees. The first level of regulation is the localization of the sensors in the cytosol where viral genomes are often found inside the cell (5, 12). The second level of regulation is the potential preference of the sensors for virus-associated structural patterns, conformations or modifications that are less common or absent in host

nucleic acids. The third level is amount of the ligand available to the sensors. If the amount of ligand is below a certain threshold, there will not be enough ligand around to trigger a robust response. As such, several nucleases and other enzymes have been identified that can negatively regulate ligand levels, many of which are inducible by type I interferons (Fig 1.2). Thus, when ligand levels escape the effect of these regulatory enzymes, they induce type I interferons thereby increasing the same effectors and helping clear viral genomes. Increasing the levels of these effectors helps eliminate infection and resolve the inflammation that is a result of the detection. Removal of any level of regulation can have devastating results for the host.

Aicardi-Goutières Syndrome

In 2008, the first reported mechanism for an inflammatory disorder that is a result of improperly regulated cytosolic nucleic acid sensing was described by Stetson, et al.(13) They showed that mice lacking Three Prime Repair Exonuclease 1 (TREX1) have an inappropriate and chronic production of type I interferons (IFN) through activation of the STING-mediated interferon-stimulatory DNA (ISD) pathway(14). Previously, mutations in TREX1 were identified as causing the human disease, Aicardi-Goutières Syndrome (AGS)(15). AGS is a monogenic autosomal recessive disorder, which can be caused by mutations in any of seven identified genes: TREX1, the three subunits of RNaseH2 (A, B or C) (16), SAMHD1 (17), ADAR1 (18) or MDA5 (19). Four of the seven are interferon-stimulated genes. AGS is classically characterized by severe encephalopathy, calcification of the basal ganglia and white matter, and lymphocyte infiltration into the cerebrospinal fluid (20-22). Interestingly, these symptoms are clinically indistinct from a congenital infection, such as CMV, and are associated with the presence of an interferon signature (23).

RNA Editing

RNA editing is the term used to describe site-specific changes to the RNA sequence resulting a difference in the transcribed RNA from the DNA template. Specifically, it refers to

the conversion of single bases to another. Many kinds of RNA have been reported as targets of editing, including tRNA, mRNA, miRNA, and rRNA (24). Deaminations in RNA are effected by a superfamily of RNA deaminases, the members of which are conserved, to some degree, throughout all life forms. Phylogenetic analysis suggests that the first members to appear in this superfamily are the RNA cytidine deaminases (CDARs), which catalyze the conversion of cytosine to uridine. This subfamily is familiar to many immunologists because it contains members of the APOBEC family and the related DNA cytidine deaminase Activation-induced Deaminse (AID). The RNA-dependent adenosine deaminases are thought to have evolved from the CDARS, with the earliest member being the Adenosine DeAminase that edits tRNA (ADAT) that is conserved and essential in Bacteria and Eukarya (25). ADATs deaminate the anti-codons of tRNAs, the effect of which increases the decoding capacity of tRNAs. Deamination of adenosine creates the non-canonical base inosine (also known as hypoxanthine). It should be noted that nucleoside deamination has arisen twice in evolutionary history. There is a second superfamily of deaminases that act on mononucleosides. Like the RNA deaminases, cytodine deaminase (CDA) evolved first followed by adenosine deaminase (ADA)(26). This family is also familiar to immunologists as one of the forms of Severe Combined Immune Deficiency (SCID) known as “boy in the bubble syndrome” is the result of ADA1-deficiency [OMIM102700]. From here out, this introduction will focus specifically on the Adenosine DeAminases that act on dsRNA, which are known as the ADARs (Fig 1.3)(27).

ADARs have been shown to edit pre-mRNAs (28), noncoding RNAs and viral RNAs. The addition of inosine to a transcript plays several roles in post-transcriptional gene regulation. Inosine is translated as guanosine, and as such, editing can remove stop codons, result in differential splicing, add premature stop codons or cause changes in the resulting amino acid sequence. Furthermore, inosine has a lower affinity for uracil than adenosine, and the addition of multiple inosines to a transcript causes destabilization of the secondary structure resulting in

degradation and elimination of the RNA. ADARs are highly conserved in metazoans, though the number of genes and isoforms differs between species. Mammals have three ADARs: ADAR1 (*ADAR*), ADAR2 (*ADARB1*) and ADAR3 (*ADARB2*). Interestingly, the *ADAR* gene has two isoforms that are the result of alternative initiation from separate promoters (Fig 1.4). The shorter ADAR1 p110 is constitutively expressed and contains double-stranded RNA binding domains (dsRBD), a deaminase domain and a nuclear retention signal. In addition to the domains found in p110, the longer ADAR1 p150 contains a nuclear export signal and two N-terminal Z-DNA binding domains (29),(30). The unique promoter for the p150 isoform is interferon inducible, suggesting a role for ADAR1 p150 in antiviral immunity (Fig 1.4).

Mutations in ADAR1 are associated with two human diseases: Aicardi-Goutieres (as mentioned previously) and Dyschromatosis Symmeterica Herediteria. There are 20 reported AGS-associated mutations found throughout ADAR1, the majority of which are in the deaminase domain, but do not effect the expression or the editing ability of the enzyme (18). Additionally, more than 130 mutations found throughout ADAR1 have been associated with Dyschromatosis Symmeterica Herediteria, a discoloration of the skin (18). Interestingly, *Adar*$^{-/-}$ mice, which lack both p110 and p150, exhibit embryonic lethality by E12.5, have an aberrant type I interferon (IFN) response and hematopoietic failure leading to liver disintegration (31, 32).

Upon the discovery of the existence of RNA adenosine deaminases, Bass and Weintraub postulated that the "unwinding/modifying activity works in concert with an as yet undetermined cellular pathway. In future experiments we hope to determine the actual pathway involved as well as the biological function and substrate for this activity" (33). Despite extensive research into ADARs, the role of ADAR1 in mammalian development and immune regulation remains uncharacterized, in large part because of the early embryonic lethality of ADAR1-deficient mice. In this thesis, I communicate the experiments we undertook in hopes of contributing to the understanding of ADAR1 biology.(34)

Chapter 1 Figures

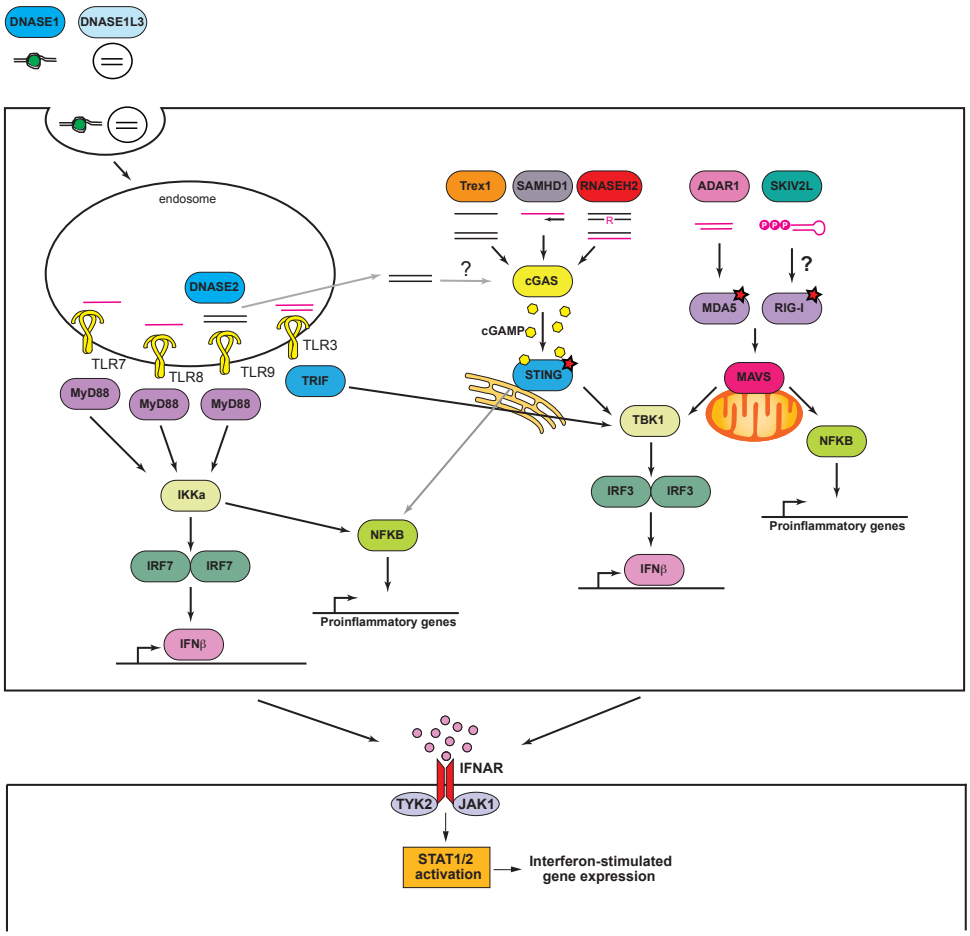

Figure 1.1: Innate pathways of viral nucleic acid detection and their negative regulators

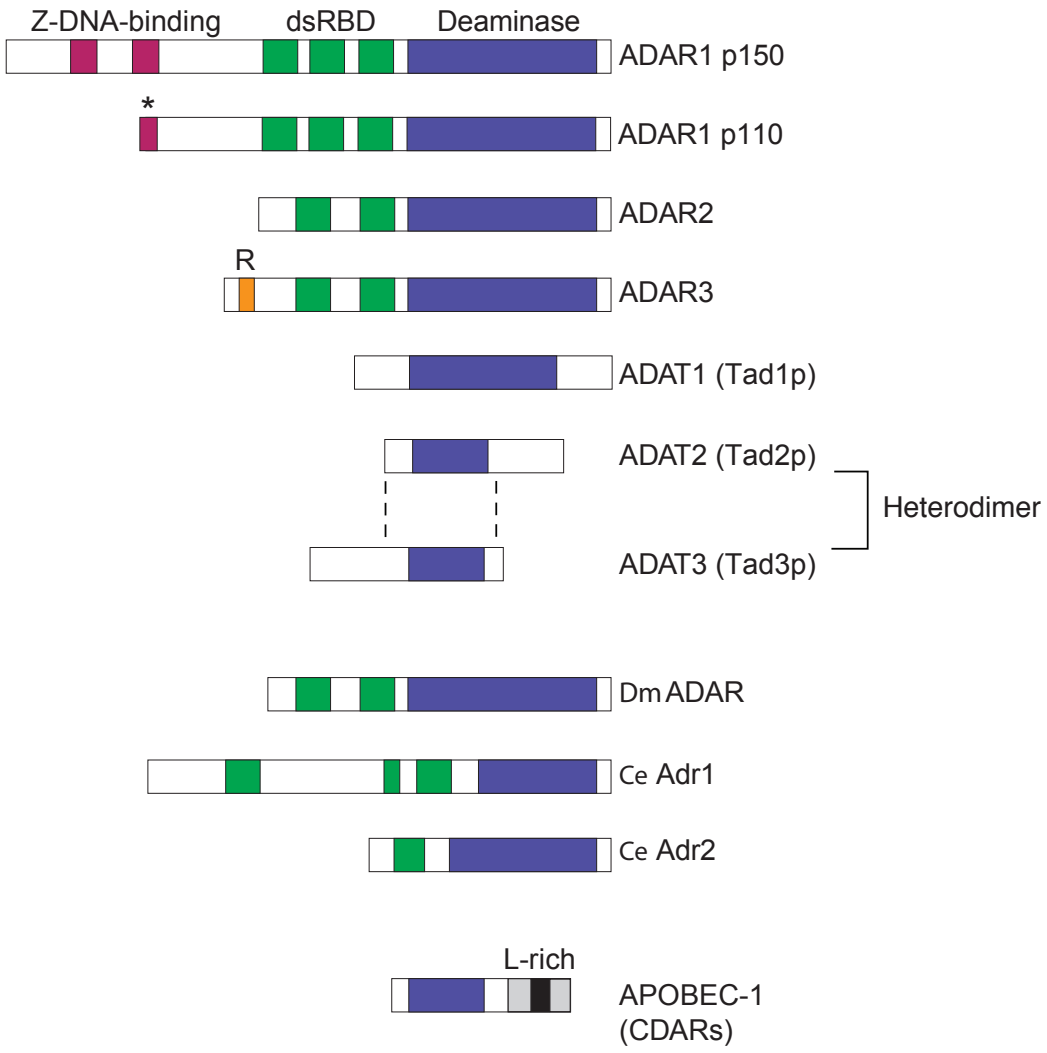

Figure 1.2: Domain structure of adenosine and cytidine deaminases acting on RNA

(a) Mammalian ADARs: ADAR1-3 and ADAT1-3. Asterisk denotes partial Z DNA binding motif that is retained in ADAR1 p110. It is missing amino acids thought to be essential for Z-DNA binding. **R** denotes arginine-rich domain.
(b) Vertebrate ADARs: *Drosophila melanogaster* and *Caenrhabditis elegans*
(c) Mammalian CDAR structure of APOBEC-1. L-rich is leucine rich domain (LRR).

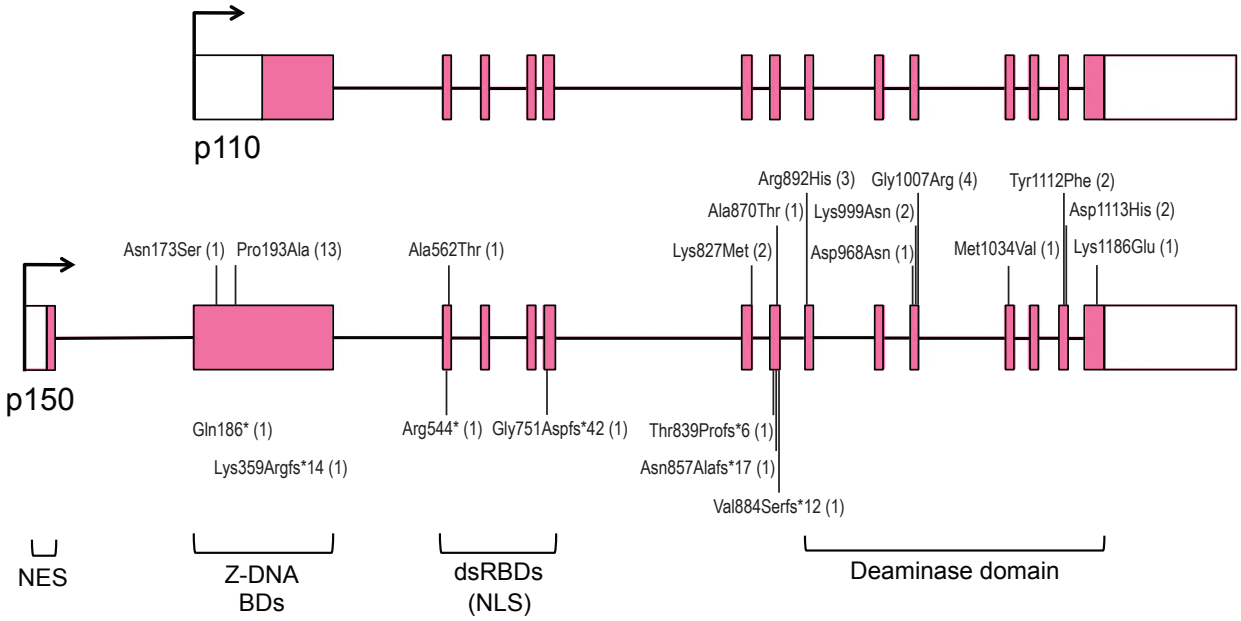

Figure 1.3: Isoforms of ADAR1 and Aicardi-Goutières Syndrome-associated mutations

Adapted from Crow, Chase (21)

Chapter 2: ADAR1 deficiency leads to an aberrant IFN response via MDA5-MAVS and negative regulation of this pathway by ADAR1 is required throughout life

Introduction

A large part of antiviral immunity is dependent on nucleic acid sensing by so-called Pattern Recognition Receptors. The first antiviral PRRs to be discovered were the endosomal Toll-Like Receptors that are expressed primarily within phagocytic cells of the immune system and detect extracellular viral genomes. However, the majority cells of cells in the body are not of hematopoietic origin and cannot phagocytosis viral particles. Furthermore, not all organisms have distinct immune cells, yet they are also susceptible to viral infections that need to be detected and eliminated. From the perspective of the virus, direct interaction with immune cells is not looked upon favorably and many viruses infect non-hematopoietic cells. Thus, there are nucleic acid pattern recognition receptors that are expressed in the majority of cells in the body and allow infected cells to mount an immune response without being an immune cell.

Cytosolic DNA is sensed by cGAS and signals through the adapter STING. Cytosolic RNAs are recognized by either of the RIG-I-like Receptors and signal through their adapter MAVS. The two pathways converge downstream of the adapters to induce IRF3- and NFkB-dependent gene expression. The major product of these pathways is the production of type I interferon and interferon-stimulated genes with contributions of other inflammatory cytokines and chemokines like TNFα, IL-6, CXCL10, CXCL1/2. The production of these signaling molecules alert neighboring cells to the presence of infection, recruit immune cells to the site of infection and can also act in an autocrine fashion on the primary infected cell. The result of the antiviral response is the elimination of the infected cells and, with them, the virus its self. Due to the inflammatory and potentially lethal consequences, it is necessary to tightly regulate this response to prevent unnecessary damage to the host.

The first negative regulator of the cytosolic nucleic acid receptors identified is Three Prime Repair Exonuclease1 (TREX1). The absence of TREX1 in mice causes the aberrant production of type I interferons and results in a lethal autoimmune disease. In humans, TREX1 is also the first gene identified to cause Aicardi-Goutières Syndrome, a severe inflammatory disorder that results in psychomotor retardation and a reduced lifespan. Six other genes have been identified to cause this rare human disease. Of the seven AGS genes, five are now known regulators of the cGAS-STING interferon stimulatory DNA (ISD) pathway. When we started this project, the most recently identified AGS gene was *ADAR,* which encodes the ADAR1 proteins. Given that the other genes could be (and are) negative regulators of the ISD pathway, how was deficiency in an RNA-editing enzyme leading to the same aberrant type I interferon production and pathology?

Very little was known about the biological roles of ADAR1 at the time. The first ADAR1-deficient mouse was published in 2000 by the Nishikura lab and exhibited a heterozygote lethality phenotype(35). However, they targeted only exons 12 and 13, and it is now hypothesized that the targeting results in a mutant protein with dominate negative effects. In 2003, the Seeburg group published a true ADAR1-deficient mouse with the homozygous null mice having an embryonic lethal phenotype by day 13.5 (with no observable phenotype in the heterozygotes)
(31). They reported that the embryos died from “liver disintegration” due to hematopoietic cell loss and massive cell death due to apoptosis. In 2009, while investigating this hematopoietic phenotype, the Orkin lab reported that E11 *Adar*$^{-/-}$ embryos exhibited a “widespread failure to appropriately regulate an interferon response”, yet assert that the lethality is due to the necessity for ADAR1 in hematopoiesis (32).

In light of the discovery that ADAR1-deficiency was associated with AGS, a disease caused by dysregulated DNA sensing, and the presence of Z-DNA binding domains and RNA-

binding domains in the ADAR1 protein we wondered if ADAR1 could be eliminating cytosolic DNA, perhaps in the form of RNA:DNA hybrids. However, given the fact that the known role for ADARs is RNA editing, was it possible that AGS could also be caused by dysregulated RNA sensing through the RLRs? Using the ADAR1-deficient mice and genome engineering in human cells, we show that ADAR1 regulates the MAVS-dependent pathway with no role for STING-dependent signaling. Furthermore, we discovered that ADAR1 is a direct negative regulator of MDA5 RNA detection and not RIG-I. Finally, we found that acute deletion of ADAR1 in 8-week-old mice causes a massive systemic inflammatory disorder to which all of the mice succumb. Whatever endogenous RNA species is triggering MDA5 in the absence of ADAR1 is present during development, as seen in the embryos, and also in adult animals.

Results

ADAR1 regulates the MDA5-MAVS signaling pathway

To determine whether ADAR1 regulates the RNA or DNA sensing pathway, we crossed the *Adar*$^{-/-}$ mice to either *Tmem173 (Sting)*$^{-/-}$ or *Mavs*$^{-/-}$ mice to generate double knockout mice. We harvested embryos at day 11.5 post fertilization, and measured the relative expression of six interferon-stimulated genes (ISGs): IP-10, ISG15, IFIT1, IFIT2, RSAD1, and MX-1. *Adar*$^{-/-}$ embryos had elevated expression of all six ISGs (Fig. 2.1a), consistent with previously published reports(32). We found that *Adar*$^{-/-}$*Sting*$^{-/-}$ mice maintained a similarly elevated IFN signature (Fig. 2.1a). In contrast, MAVS deficiency completely restored the expression of all six ISGs to control levels (Fig. 2.1a). Thus, the aberrant interferon response in *Adar*$^{-/-}$ embryos is completely dependent on MAVS signaling, which was recently reported(36). Furthermore, we compared the litters from intercrossing *Adar*$^{+/-}$*Sting*$^{-/-}$ or *Adar*$^{+/-}$*Mavs*$^{-/-}$ mice to those generated by intercrossing *Adar*$^{+/-}$ mice. We recovered no live *Adar*$^{-/-}$*Tmem173*$^{-/-}$ mice. However, we found that all *Adar*$^{-/-}$*Mavs*$^{-/-}$ mice survived past birth (Fig 2.1b). We became the

first group to show that MAVS signaling is entirely responsible for the embryonic lethality of *Adar*$^{-/-}$ mice.

To further explore this result, we crossed the *Adar*$^{-/-}$ mice to the either of the individual RIG-I-like receptor knockout mouse lines (*Ifih1*$^{-/-}$ [MDA5] or *Ddx58*$^{-/-}$ [RIG-I]). We intercrossed *Adar*$^{+/-}$*Ifih1*$^{-/-}$ mice and *Adar*$^{+/-}$*Ddx58*$^{+/-}$ mice and harvest embryos 11.5 days post-fertilization. We evaluated expression of interferon-stimulated genes (ISGs) across the various genotypes and found that deficiency in MDA5, but not RIG-I, restored ISG expression to the level of *Adar*$^{+/+}$ (Fig 2.2a). We evaluated the live births on the *Ifih1*$^{-/-}$ background and found no differences between the *Adar*$^{-/-}$*Mavs*$^{-/-}$ mice and the *Adar*$^{-/-}$*Ifih1*$^{-/-}$ mice (Fig 2.2b). This shows that that ADAR1 is a specific negative regulator of the MDA5-MAVS pathway and not RIG-I-MAVS. It also plays no role in regulating the STING-pathway.

To investigate whether the role for ADAR1 in the regulation of cytosolic sensing of RNA is required throughout life, and not just during embryogenesis and development, we crossed floxed-*Adar* mice to *UBC:Ert2Cre* transgenic mice that express a tamoxifen-inducible Cre in all tissues under the control of the human ubiquitin promoter. After 3 doses of tamoxifen (Fig 2.3a), all the mice died from a lethal inflammatory disorder (Fig 2.3b) characterized by increased serum cytokines (Fig 2.3c), hypothermia (Fig 2.3d), and vascular leakage. It should be noted we only reported 16 cytokines in the text of the paper. I am reporting all 30 cytokines here. The majority of the issues we observed histologically were in the intestines, with severe breakdown of the barrier and inflammatory infiltrates. Unfortunately, a proportion of that inflammation was due to the activation of the Ert2Cre, itself, as we observed a similar but less severe phenotype in *Adar*$^{+/+}$*UBC:Ert2Cre*$^{Tg/+}$ mice that were treated simultaneously with tamoxifen.

Regulation of MDA5-MAVS by ADAR1 is required in human cells

To address the role of ADAR1 in human cells, we used Cas9/CRISPR (Clustered Regularly Interspaced Short Palindromic Repeats) to target the ADAR gene. We designed a guide RNA to target exon 4, which is present in both the p110 and p150 isoforms of ADAR1. We transduced human HEK293T cells with a lentivirus expressing an ADAR-targeting gRNA and the Cas9 endonuclease, selected cells in puromycin for three days and single cell cloned the surviving cells. Wild type and mutated alleles can be distinguished based on the disruption of a restriction digest site located within the gRNA sequence. We recovered several clonal lines of 293T cells with complete modification of *ADAR* alleles, as shown by resistance of the CRISPR-targeted, PCR-amplified region of genomic DNA to ApoI digestion (Fig 2.4a, "NHEJ" band").

We evaluated ADAR1 protein expression by western blot in a representative clone of targeted 293T cells. Control 293T cells transduced with Cas9 alone expressed constitutive levels of p110 protein, as well as IFN-inducible p150 ADAR1 (Fig 2.4b). In contrast, one of our targeted 293T clones (#10) completely lacked expression of either isoform of ADAR1, demonstrating complete disruption of all alleles of the ADAR gene in human cells (Fig 2.4b), which we confirmed by Sanger sequencing of the three mutations in the three alleles on ADAR in 293Ts (Fig 2.4c). When we overexpressed increasing amounts of either RIG-I or MDA5 in the presence of an interferon-stimulatory response element driving the expression of luciferase, we found that the *ADAR*null 293T cells were hyper-responsive to MDA5-expression and not RIG-I as compared to both parental 293T (untargeted), as well as a *ADAR*-sufficient clone (Fig 2.5). The *ADAR*null 293Ts confirm that ADAR1 specifically regulates the MDA5-MAVS signaling pathway in both mice and humans.

Embryonic lethality due to MAVS signaling is the result of more than just IFNAR1 and TNFR1 signaling

Finally, we briefly interrogated what signaling downstream of MAVS is required for the embryonic lethality. We have shown previously that the autoimmunity that results in the absence of Trex1 is completely rescued on a type 1 interferon receptor (IFNAR1)-deficient background. Acute deletion of ADAR1 in adults results in the induction of a variety of inflammatory cytokines in the serum in addition to type I IFN. It has also been shown that MAVS activation results in a robust NFkB-dependent signaling, a pathway that appears to be weaker downstream of cGAS/STING (refs). Thus, we cross the ADAR1-deficient mice to IFNAR1-, TNFR1-, RIPK3-deficent mice or combinations thereof. We have determined that IFNAR1-deficiency, TNFR1-deficiency, nor RIPK3-deficiency (Tayla Olsen, Oberst Lab) alone can rescue the embryonic lethality (Fig 2.6). The combination of IFNAR1 and TNFR1 deficiencies is also unable to rescue. In is possible that TNFR2 is playing a role in lethality given its expression in the gut and the role for ADAR1 in gut development and homeostasis, but this remains to be addressed. However, we can say that type I IFN signaling alone is not responsible for the inflammation and death observed in the absence of ADAR1, unlike TREX1-deficiency.

Discussion

Our findings reveled that ADAR1 is a specific negative regulator of MDA5/MAVS dependent signaling. We have also revealed that the embryonic lethality observed in *Adar*-deficient mice is entirely a result of aberrant MAVS signaling. The fact that ADAR1 has an exclusive relationship with MDA5 and not RIG-I suggests that a distinct group of RNAs is targeted for regulation. From the beginning of this project, we have hypothesized that some kind of endogenous ligand was responsible for the type I IFN signature that occurs in the *Adar*-deficient mice and the AGS patients with ADAR1 mutations. We have employed various methods to detect the relevant RNA, including total RNA sequencing in the *Adar*-deficient embryos, transfection of RNAs from *Adar*-deficient embryos or *ADARnull* 293Ts into macrophages, and the overexpression of MDA5 in *ADARnull* 293Ts driving the expression of luciferase in an ISRE-dependent manner. However, each of these experiments had many caveats and none of these methods have definitively identified the endogenous MDA5 ligand. Moving forward we will use two different sequencing approaches in the *ADARnull* 293Ts: iCLIP-seq and TRIBE-seq. Both methods are target-enrichment strategies and should be more effective than previous attempts as they depend on the specific relationship between ADAR1 and MDA5

Our data shows that the endogenous ligand that is regulated by ADAR1 is present in both embryos and adult cells. The rapid decline of the induced knockouts precludes us from determining if there is a specific cell type (or types) that is the primary responder to the endogenous ligand. The toxicity to the gut of both ADAR1-deficiency and ERT2-Cre activation also prevent us from determining a role for the cellular immune system in this response, including whether the adaptive immune system is required. However, given the fact that MAVS-dependent inflammation is responsible for embryonic lethality at such an early time point, it is unlikely that the adaptive immune system plays a significant role in this disease.

When we embarked on the project, it was considered unlikely that two pathways would lead to one disease, and specifically, that endogenous RNA ligands would exist (Hannah and Dan's review). This data highlights an interesting difference between the *Trex1* and *Adar* deficiencies. Mice lacking TREX1 succumb to a lethal autoimmune cardiomyopathy, but the ADAR1-deficient mice succumb to a lethal autoinflammatory disease. And yet, AGS as a result of TREX1 mutations is induced earlier and is slightly more lethal than AGS as a result of ADAR1 mutations. Thus a few questions remain unanswered: Are the observed differences due to the nature or expression pattern of the different ligands? Are they the result of differences in the signaling pathways downstream of STING or MAVS? Or, perhaps, other forms of regulation of those two pathways? It is possible that null mutations in human ADAR1 cause significantly stronger inflammation resulting in embryonic lethality as compared to the currently known ADAR1 AGS mutations that neither prevent expression nor observable function of the enzyme. Unfortunately, the analysis of the catalytically inactive ADAR1 mutant mice reported by Walkley, *et a*l, leaves a lot to be desired, but could provide more insight into these questions if they were fully examined.

Chapter 2 Figures

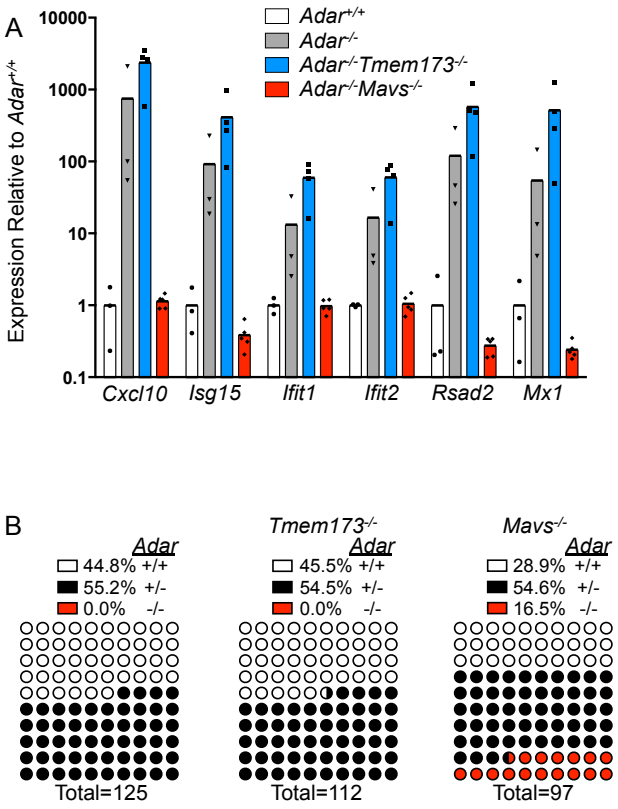

Figure 2.1: ADAR1 is a negative regulator of MAVS signaling.

(a) Quantitative RT-PCR on a panel of six ISGs from whole E11.5 embryos. *Adar*$^{+/+}$ (white, n = 3), *Adar*$^{-/-}$ (grey, n = 3), *Adar*$^{-/-}$*Sting*$^{-/-}$ (blue, n = 4), *Adar*$^{-/-}$*Mavs*$^{-/-}$ (red, n = 5). Interferon signature assessed by Wilcoxon signed rank test compared to *Adar*$^{+/+}$: *Adar*$^{-/-}$ p = 0.03, *Adar*$^{-/-}$*Sting*$^{-/-}$ p = 0.03, *Adar*$^{-/-}$*Mavs*$^{-/-}$ p = 0.31.
(b) Live births from *Adar*$^{+/-}$, *Adar*$^{+/-}$*Tmem173*$^{-/-}$, or *Adar*$^{+/-}$*Mavs*$^{-/-}$ intercrosses. Percent rescue p > 0.05 by chi square goodness-of-fit

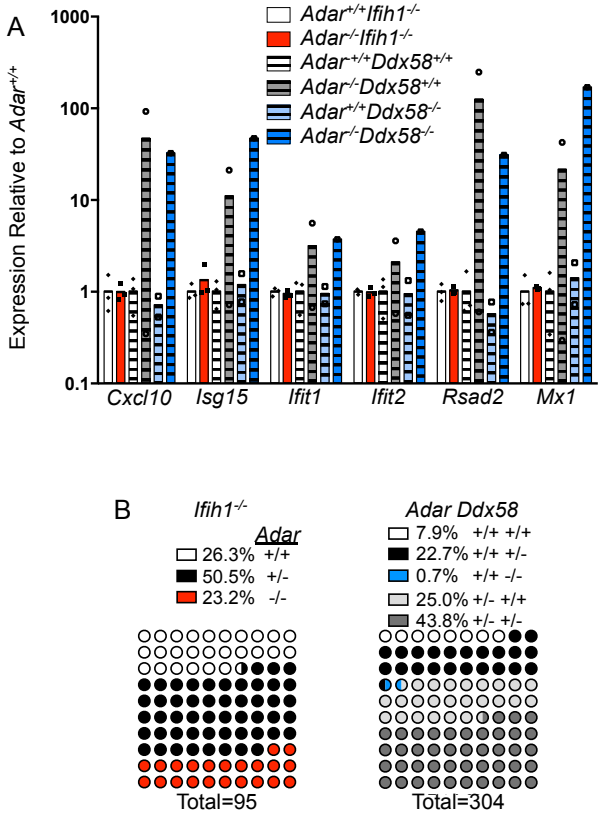

Figure 2.2: ADAR1 is, specifically, a negative regulator of MDA5 signaling

(a) Quantitative RT-PCR on a panel of six ISGs from whole E11.5 embryos. *Adar*$^{+/+}$*Ifih1*$^{-/-}$ (white, n = 3), *Adar*$^{-/-}$*Ifih1*$^{-/-}$ (red, n = 3), *Adar*$^{+/+}$*Ddx58*$^{+/+}$ (white stripes, n = 3), *Adar*$^{-/-}$*Ddx58*$^{+/+}$ (gray stripes, n = 2), *Adar*$^{+/+}$*Ddx58*$^{-/-}$ (light blue stripes, n = 2), *Adar*$^{-/-}$*Ddx58*$^{-/-}$ (blue stripes, n = 1). Interferon signature assessed by Wilcoxon signed rank test compare to *Adar*$^{+/+}$ controls, *Adar*$^{-/-}$*Ifih1*$^{-/-}$ p = 0.56, *Adar*$^{-/-}$*Ddx58*$^{+/+}$ p = 0.03, *Adar*$^{+/+}$*Ddx58*$^{-/-}$ p = 0.69, *Adar*$^{-/-}$*Ddx58*$^{-/-}$ p = 0.03.

(b) Live births from *Adar*$^{+/-}$*Ifih1*$^{-/-}$ or *Adar*$^{+/-}$*Ddx58*$^{+/-}$ intercross. Percent rescue p > 0.05 by chi square goodness-of-fit

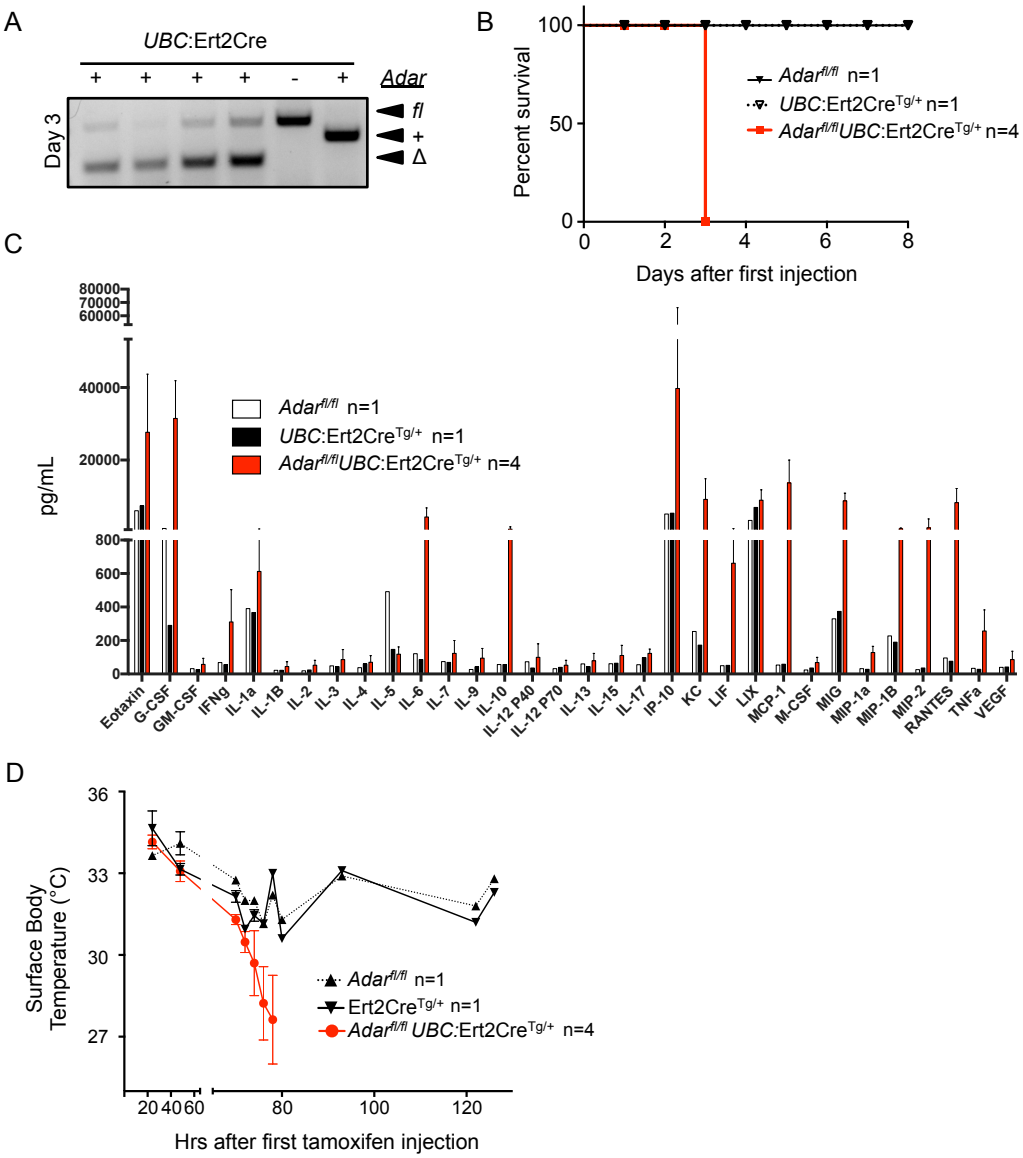

Figure 2.3: Negative regulation of MAVS signaling by ADAR1 is required in adult animals.

Mice were treated with 2 mg tamoxifen i.p. daily for 3 days and observed for gross pathology.

(a) Samples of the ear were genotyped for *Adar* deletion after tamoxifen treatment

(b) Surivial curve for mice treated with tamoxifen

(c) Serum cytokine levels determined from mice at day 3

(d) Surface body temperate readings for tamoxifen-treated mice at 20–120 hr after initial tamoxifen injection

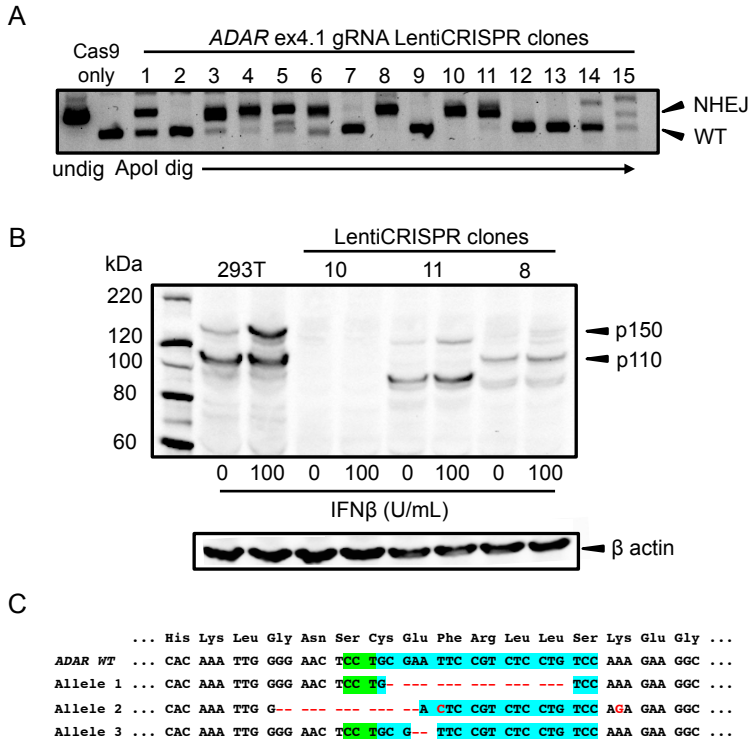

Figure 2.4: Generation of ADARnull HEK293T cells by LentiCRISPR targeting

(a) Transduction of HEK293T cells with *ADAR*-gRNA-Cas9 lentivirus results in complete targeting of the *ADAR* locus in several single cell clones as measured by resistance of the genome to enzymatic digestion at the site of the guide targeting sequence.

(b) Immunoblot of ADAR1 protein using lysates from control HEK293T cells and three clones that were observed to have complete targeting at the genome level.

(c) Genotype of CRISPR target site in *ADAR*-lentiCRISPR-targeted clone 10. The CRISPR target site in exon 4 of *ADAR* is indicated in blue, and the protospacer adjacent motif (PAM) is shown in green. Deletions in all three alleles, each of which results in a frameshift, are shown by the red dashes.

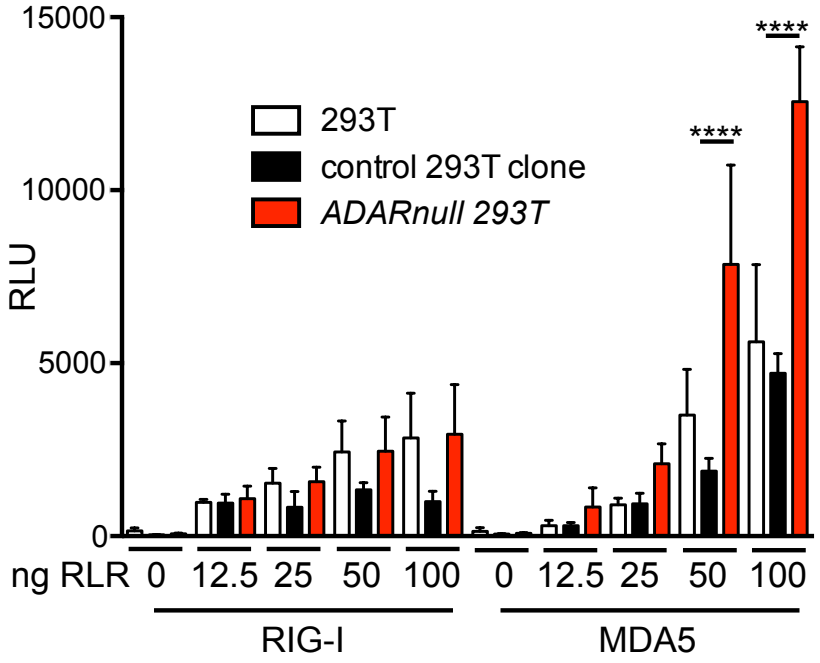

Figure 2.5: ADAR1 specifically regulates the MDA5 pathway in human cells

a) The indicated HEK293T cells were transfected with 25 ng ISRE-luciferase reporter plasmid, with or without the indicated amounts of plasmid encoding RIG-I or MDA5. Cells were analyzed for relative luciferase units 24 hr after transfection. Mean ± SD; ***p < 0.0001 in two-way ANOVA test with Tukey's multiple comparison. Data are representative of four independent experiments.

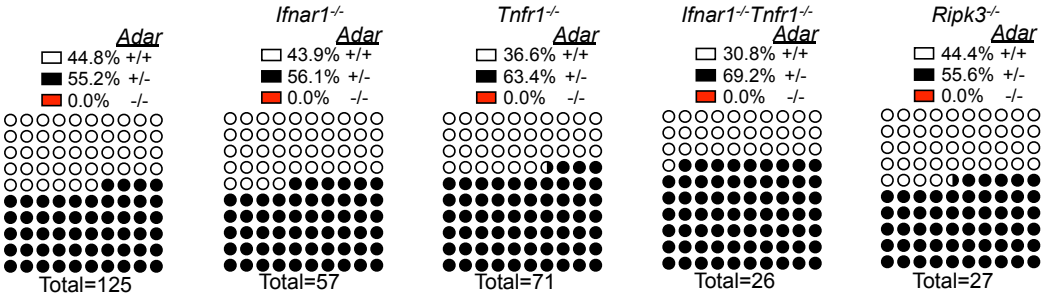

Figure 2.6: Adar-deficiency is not rescued by deficiencies in IFNAR1, TNFR1, RIPK3, nor IFNAR1 and TNFR1

(a) Live births from *Adar*$^{+/-}$*Ifnar*$^{-/-}$, *Adar*$^{+/-}$*Tnfr1*$^{-/-}$, *Adar*$^{+/-}$*Ifnar*$^{-/-}$*Tnfr1*$^{-/-}$, or *Adar*$^{+/-}$*Ripk3*$^{-/-}$ intercrosses. Percent rescue $p > 0.05$ by chi square goodness-of-fit. The *Adar*$^{+/-}$ intercross is shown here, again, for reference. Ripk3 cross performed and analyzed by Tayla Olsen in Oberst Lab.

Chapter 3: ADAR1 is required for normal development of cells and organs

Introduction

Brenda Bass and Harold Weintraub discovered ADARs in 1987 when trying to use RNA interference in Xenopus embryos (37). The technique worked well in oocytes, but embryos required injections of 1000-fold excess of the antisense RNA in order to see decreases in the target RNA. Unlike oocytes, the duplex of sense-antisense RNA was "unwound" within half an hour of formation in the embryos. They further show that the process only affects double stranded RNA, is not inhibited by ssRNA, ssDNA or dsDNA and is susceptible to Proteinase K treatment. They had discovered a double stranded RNA "denaturase". The next year they showed that the dsRNA is never fully unwound (33) and the unwinding results in a covalent change such that the targeted RNA no longer pairs as before. They identified that the change they observed was the inclusion of inosine into the target RNA. Thus, the breakdown of the dsRNAs into ssRNAs they observed before wasn't truly the result of "denaturing"; rather, the enzyme was modifying adenosine to inosines and the double stranded structures were no longer viable through base pairing.

Several targets of editing enzymes had been discovered at the same time the enzymes themselves were being identified. The first example of editing in a nuclear RNA was the discovery of the conversion of cytidine 6666 in apolipoprotein B mRNA to uridine in 1987 (38), (39). This deamination by APOBEC1 converts a glutamine codon to a stop codon resulting in two isoforms of the apoB protein with distinct expression patterns and roles in lipid metabolism. The first identification of an adenosine deamination event in an RNA is still the most famous. In 1991, the Seeburg group reported (40) the editing of the Q/R site in the AMPA-selective glutamate receptor GluRB. Mice that have un-editable GluRB, either by lacking the editing site (deltaQ) or having an asparagine in place of the glutamine (Q>N), are severely runted and suffer from seizures before succumbing by ~20 days of age (41) (42). Similarly, ADAR2-deficient mice

have the same phenotype and are completely rescued by biallelic knock-in of the “edited” form (Q>R) or GluRB (43). Furthermore, ADAR-deficient *Drosophilia* exhibit adult-stage incoordination and temperature sensitive paralysis (44) and *adr* mutant *C. elegans* have chemotactic defects and a reduced lifespan (45) (46). These findings show that ADARs and RNA editing have critical roles in biology, but what role does ADAR1 play, specifically?

Using mice that constitutively lack both ADAR1 and the aberrant inflammation due to its absence, we discovered previously unknown roles for ADAR1 in organogenesis, B cell development and tissue homeostasis. Further explorations of these phenotypes revealed that the B cell phenotype observed in the absence of ADAR1 and MAVS is intrinsic to the B cells using *Mb1*-Cre knock-in mice. We found that ADAR1 is required in B cells for proper maturation of pro-B cells to pre-B cells. Finally, using inducible deletion on a MAVS-deficient background we found that ADAR1 expression is required to maintain tissue homeostasis in the intestine and without ADAR1 half of the mice succumb within 8 days of deletion. Together these data show specific and previously unknown roles for ADAR1 in biology.

Results

The elimination of the IFN signature and the live births of *Adar*$^{-/-}$*Mavs*$^{-/-}$ mice enabled the analysis of the role of ADAR1 in development independent from the pathological IFN response. The *Adar*$^{-/-}$*Mavs*$^{-/-}$ mice that survived past the first two days after birth (Fig 3.1a) were severely runted compared to their *Adar*$^{+/+}$*Mavs*$^{-/-}$ littermates (Fig 3.1b). We euthanized mice at 20 days of age and performed a full necropsy and histological analysis, comparing three *Adar*$^{+/+}$*Mavs*$^{-/-}$ littermates to three *Adar*$^{-/-}$*Mavs*$^{-/-}$ mice. We found that despite their runted stature, the *Adar*$^{-/-}$*Mavs*$^{-/-}$ mice were feeding, as they had stomachs full of milk. However, we uncovered a number of previously unknown developmental phenotypes in the double knockout mice, revealing a novel role for ADAR1 in development that is distinct from its role in regulation of the MAVS-dependent antiviral response. First, we found that kidneys of *Adar*$^{-/-}$*Mavs*$^{-/-}$ mice were multipapillary and hydronephrotic, in contrast to wild-type mice that have monopapillary kidneys (Fig. 3b), suggesting a critical role for ADAR1 in regulation of organ patterning during development. Next, we noticed that the gastrointestinal tract in *Adar*$^{-/-}$*Mavs*$^{-/-}$ mice was severely disorganized, with vacuolated and disrupted epithelial cells, together with inflammatory infiltrates (Fig 3.1c). This phenotype was strongest in the small intestine and milder in the distal colon. We found a lack of lymphoid follicles in lymph nodes and spleens of *Adar*$^{-/-}$*Mavs*$^{-/-}$ mice, together with a severe reduction in B cells (Fig 3.1c-e). However, T cells and myeloid cell numbers were relatively normal in spleen and thymus (Fig 3.1e and not shown). These findings suggest a selective role for ADAR1 in the regulation of B cell development.

Additionally, we analyzed bone marrow, blood and splenocytes from an *Adar*$^{-/-}$*Mavs*$^{-/-}$ mouse for hematopoietic progenitor populations. We found that Adar-deficient mice have relatively normal hematopoietic development with slight differences in the myeloid progenitor compartment. We saw an increase in GMPs and a reduction in MPP, but no difference in any of the other major subsets, including CLPs (Fig 3.2a). The *Adar*$^{-/-}$*Mavs*$^{-/-}$ mouse had elevated

progenitors in the blood and spleen (fig 3.2b-c, consistent with extramedullary hematopoiesis, which we also observed by histology (Fig 3.1c). These findings demonstrate that the hematopoietic failure observed by other groups in *Adar*$^{-/-}$ embryos and upon *Adar* deletion in the adult mouse hematopoietic system is largely due to abnormal activation of the MAVS-dependent antiviral response.

To further explore the MAVS-independent the roles for ADAR1, we have evaluated the B cell phenotypes of several Adar-deficient mice. We found that the major subsets of B cells in the spleen were not different between *Adar*$^{+/+}$*Mavs*$^{-/-}$ and *Adar*$^{-/-}$*Mavs*$^{-/-}$ at 15 days of age (Fig 3.3a). We further assessed the bone marrow for B cell-specific progenitors (Fig 3.3b) at 18 days old. Like the spleen, we observed a severe overall deficiency in B cells, but we did see slight differences in developmental subsets, with the most striking being a deficiency in IgM+ B cells (which subset in "mature" and "immature" based on IgD expression, both of which were reduced). A potential issue with these results is that they must be viewed in the context that the mice are 15 days old and, therefore, lack a fully developed immune system.

In an attempt to address whether the role for ADAR1 in B cells is cell intrinsic and to avoid the confounding developmental issues that the *Adar*$^{-/-}$*Mavs*$^{-/-}$ mice present, we made bone marrow chimeras transplanting either *Adar*$^{+/+}$*Mavs*$^{-/-}$ or *Adar*$^{-/-}$*Mavs*$^{-/-}$ bone marrow into congenically marked *Mavs*$^{-/-}$ hosts. We waited 8 weeks post-transplant before evaluating the bone marrow and spleen of these mice. As we see with the *Adar*$^{-/-}$*Mavs*$^{-/-}$ mice, recipients of *Adar*$^{-/-}$*Mavs*$^{-/-}$ bone marrow also had a severe B cell deficiency in the bone marrow and the periphery. The *Adar*$^{-/-}$*Mavs*$^{-/-}$ chimeras differed from the *Adar*$^{-/-}$*Mavs*$^{-/-}$ mice in the B cell subsets in the spleen. We observed a slight increase in transitional B cells and a 20% decrease in mature follicular B cells (Fig 3.4a). The phenotype of the bone marrow B cells was more dramatic. We observed a significant increase in pro B cells and a decrease in IgM+ B cells, but in this case there was a strong reduction in the IgM+IgD+ "mature" compartment (Fig 3.4b). We

had very few of these mice reconstitute due to technical issues, so this data bears repeating and should be viewed as preliminary. However, it is significantly difficult to obtain *Adar*$^{-/-}$*Mavs*$^{-/-}$ donor mice and when we do, the runted nature of the mice prevents us from transplanting very many recipients.

To avoid these issues, we used bone marrow from *Adar*$^{fl/fl}$*UBC:Ert2Cre*$^{Tg/+}$*Mavs*$^{-/-}$ mice, allowed the mice to reconstitute and then knocked out Adar acutely with a course of tamoxifen injections. Unfortunately, there was no phenotype in B cells observed in these mice (fig 3.5a-b). In fact, when we genotyped the single cell suspensions of splenocytes and bone marrow cells by PCR, we found that only 50% of the Adar alleles had recombined and also did not detect any donor alleles (Fig 3.5c). This explains why were unable to observe the typical ADAR1-dependent B cell phenotype. The ideal solution to this problem would be to cross the mice to a Cre-reporter line, allowing us to analyze only the cells that have recombined their Adar alleles. Given that the mice already carry three modified genes, the breeding required to include a Cre-reporter would be impractical.

However, we directly addressed the question of whether the deficiency in B cells that results in the absence of Adar is intrinsic to the B cells themselves by crossing floxed *Adar* mice to mice that express Cre specifically in B cells (*Mb1*, Iga). These mice exhibit a nearly identical overall phenotype as what we observed in the *Adar*$^{-/-}$*Mavs*$^{-/-}$ bone marrow chimeric mice, but with stronger significance owing, in part, to the increase in the number of mice analyzed. The bone marrow lacks B cells overall with a significant block at the pro-pre B cell stage (much like what is observed in *Btk*$^{-/-}$*Tek*$^{-/-}$ mice) (Littman 2000 jem)(Fig 3.6a). There is also a significant reduction in IgM+ B cells, with the majority being IgD-. The spleen is even more striking. Again we see a loss of total B cells, but the *Adar*$^{fl/fl}$*Mb1*$^{Cre/+}$ mice have higher percentages of T1, T2 and MZ B cells with a severe loss in the mature follicular B cell subset (Fig 3.6b). At this point we can

conclude that the loss of B cells observed in *Adar*-deficient animals is, in fact, intrinsic to the B cells rather than the result of some other defect.

When we acutely deleted *Adar* on a MAVS-deficient background (Fig 3.7a) they were protected from the severe inflammatory disorder as observed by normal body temperature (Fig 3.7b) and lack of serum cytokines (Fig 3.7c). However, eight days after the initial tamoxifen treatment 50% of the mice declined to the point of requiring euthanasia (Fig 3.7d), marked by hunching, failure to groom and severe diarrhea. Upon histological examination we found inflammation throughout full length of the intestines (stomach to colon) of all of the mice (Fig 3.7e), with the most severe inflammation found in the colon of the moribund mice (Fig 3.7f-g). Both sets of inducible knockout mice support what we observed in the constitutive knockout mouse: ADAR1 negatively regulates the MAVS pathway and is necessary for tissue homeostasis. The extent to which ADAR1 is necessary in adult mice could be further explored by treating a larger cohort of $Adar^{fl/fl}UBC{:}Ert2Cre^{Tg/+}Mavs^{-/-}$ mice with tamoxifen and observe for additional long term effects in tissues beyond the intestinal issues we observed on day eight.

Finally, in our evaluations of $Adar^{-/-}Mavs^{-/-}$ mice, we had found previously unknown roles for ADAR1 in the development and homeostasis of the kidneys and the intestines. We generated next-generation sequencing libraries from rRNA-depleted total RNA harvested from E11.5 embryos from $Adar^{+/+}$, $Adar^{-/-}$, $Adar^{+/+}Mavs^{-/-}$ and $Adar^{-/-}Mavs^{-/-}$ mice. When we compared the gene expression between the $Adar^{+/+}$ and $Adar^{-/-}$ embryos, the majority of the differentially regulated genes were ISGs (Fig 3.8a) and they were eliminated on the MAVS-deficient background (Fig 3.8b). However, we also noted the presence of a class of genes that were ADAR1-dependent but MAVS-independent (Fig 3.8c), which is supported by the developmental defects and lethality we observed in the live births of the $Adar^{-/-}Mavs^{-/-}$ and $Adar^{-/-}Ifih1^{-/-}$ mice. We performed pathway analysis on these genes and found that they were enriched for genes involved in a variety of biological pathways, with the majority of statistically

significant hits being in the transport and degradation of lipids and small molecules (Fig 3.8d). We also looked for transcription factor enrichment in these genes and found members of the WNT/TCF and HOX families (Fig 3.8e). These transcription factors are not surprising given their highly established roles in a variety of developmental pathways.

Discussion

We now have demonstrated two distinct roles for ADAR1: the negative regulation of MDA5/MAVS signaling and the regulation of multi-organ development and homeostasis. When we started this project, we were sure that we would be able to answer and address the first role, but had no idea that we would really contribute anything to the understanding of the second role. The discovery that the *Adar*$^{-/-}$*Mavs*$^{-/-}$ mice were both fully rescued to birth and capable of surviving long enough to be analyzed revealed more about the *in vivo* relevance of role ADAR1 in biology than could have been anticipated. In fact, the *Adar*$^{-/-}$*Mavs*$^{-/-}$ mice really champion the necessity of using animal models in biomedical research. Whether or not everything we have learned about ADAR1 from the *Adar*$^{-/-}$*Mavs*$^{-/-}$ mice can be extrapolated directly to human, the wealth of information they have provided is unmatched by any of the *in vitro* studies.

We now know that ADAR1 plays a significant role in kidney formation. The odd kidney patterning we observed is non-trivial. There is no known developmental defect that causes the same pathology. Thus, ADAR1 either regulates something completely novel or regulates multiple pathways in novel ways such that the combinatorial defects result in the observed kidney deformity. The precise nature of the defects could be addressed by crossing the *Adar*$^{fl/fl}$ mice to a kidney specific Cre. Another possibility is to treat larger cohorts of the *Adar*$^{fl/fl}$*UBC:Ert2Cre*$^{Tg/+}$*Mavs*$^{-/-}$ mice with tamoxifen and see if those that do not succumb to intestinal distress develop kidney disease. However, it is likely that the effects of ADAR1-deficieny on the kidney are developmentally determined and would not be observed upon acute deletion in adult animals.

The role for ADAR1 in the intestine is complicated, but consistent. We have observed it in every model; yet, several caveats exist in every model that precludes us from making any definitive statements. There is significant inflammation, apoptosis and enterocyte vacuolation in the small intestines of the *Adar*$^{-/-}$*Mavs*$^{-/-}$ mice as compared to *Adar*$^{+/+}$*Mavs*$^{-/-}$ littermates. The

problem is that at the time of analysis, the *Adar*$^{-/-}$*Mavs*$^{-/-}$ mice remain on a milk-only diet, whereas their wild-type brothers have transitioned to a diet of mainly mouse chow. Under the influence of the diet (i.e., milk to solid food), and especially after weaning, the composition of the microbiota changes rapidly which may influence the inflammation we observe in the *Adar*$^{-/-}$ *Mavs*$^{-/-}$ mice. Furthermore, it is thought that the lipids and liposomes in the milk can be mildly inflammatory on their own, further complicating our observations. Our final model, *Adar*$^{fl/fl}$*UBC:Ert2Cre*$^{Tg/+}$*Mavs*$^{-/-}$ mice, also exhibit significant levels of intestinal inflammation from the stomach through the colon. However, the role for ADAR1 in this process is impeded by the toxicity of tamoxifen in corn oil and the substantial toxicity of the activated ERT2-Cre, as we observed severe inflammation of the gut in tamoxifen-treated *UBC:Ert2Cre*$^{Tg/+}$ mice.

The mechanism behind the role of ADAR1 in B cell development is completely unknown. What we have observed in the bone marrow is reminiscent of the phenotype seen in mice with deficiencies in proximal BCR signal transduction. It's nice to hypothesize that ADAR1 may regulate some component of BCR signaling, however it is completely possible that it is the result of something else entirely. We plan to perform mRNA-seq on sorted splenic subsets from the *Adar*$^{fl/fl}$*Mb1*$^{Cre/+}$ mice. However, the splenic phenotype in these mice has not been observed in the other B cell-deficient scenarios we have analyzed. Thus, we are currently crossing the *Adar*$^{fl/fl}$*Mb1*$^{Cre/+}$ mice to *Mavs*-deficient mice to exclude any role for MAVS signaling. All further analysis of the B cell phenotypes will be done using the *Mavs*-deficient *Adar*$^{fl/fl}$*Mb1*$^{Cre/+}$ mice, including serum antibody titers and isotyping, B1 B cell analysis in the spleen and peritoneum, IF on splenic sections to visualize follicle formation, and further *in vivo* and *in vitro* tests of B cell functionality, proliferation and phenotype in both bone marrow and splenic B cells.

Chapter 3 Figures

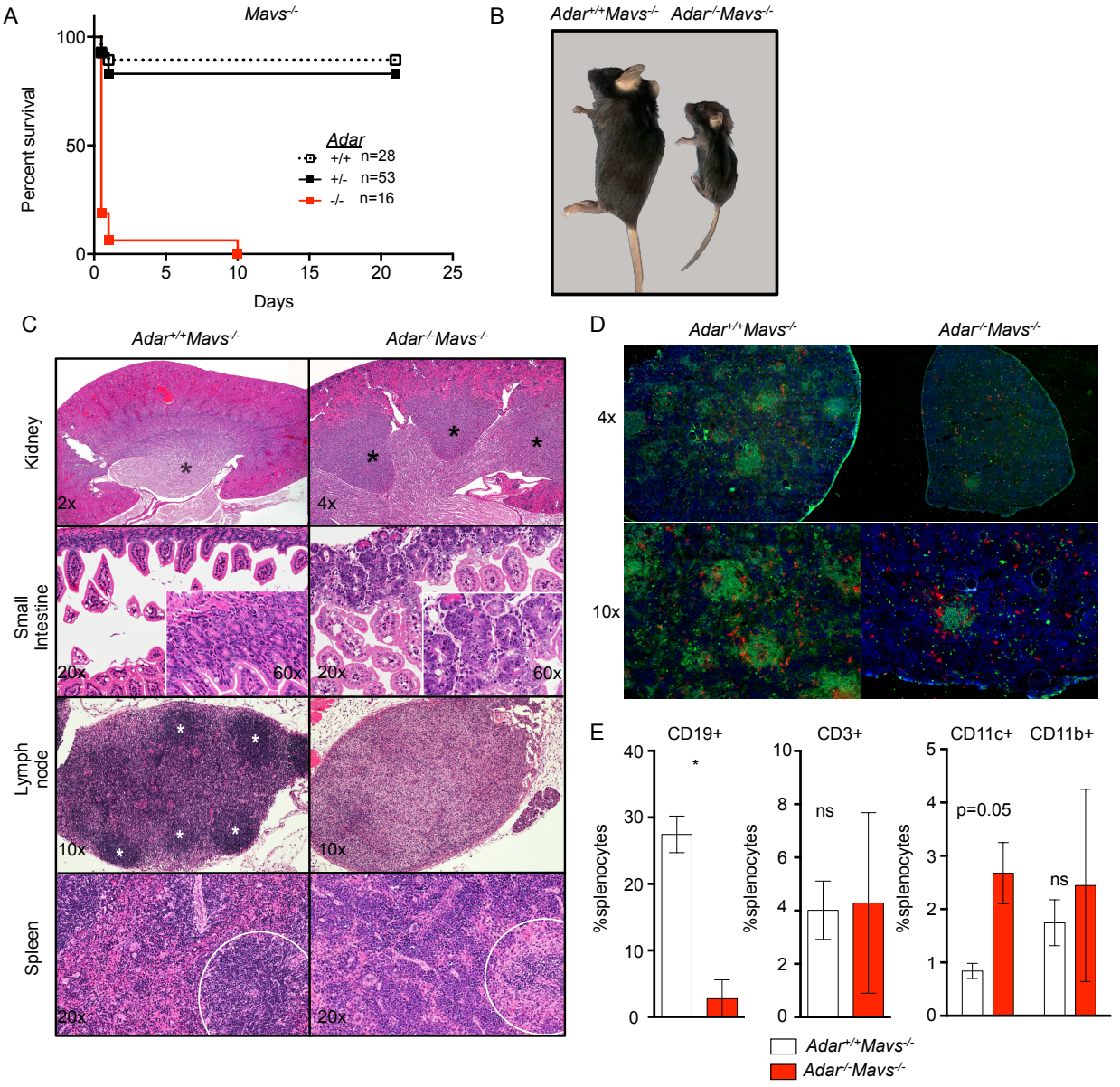

Figure 3.1: Postnatal mortality and severe developmental defects in Adar$^{-/-}$Mavs$^{-/-}$ *mice*

(a) Postnatal survival curves for *Adar*$^{-/-}$*Mavs*$^{-/-}$ mice

(b) *Adar*$^{-/-}$*Mavs*$^{-/-}$ mice are severely runted compared to *Adar*$^{+/+}$*Mavs*$^{-/-}$ littermates at 20 days old

(c) *Adar*$^{-/-}$*Mavs*$^{-/-}$ mice have developmental defects of the kidney (top row; papillae marked with black asterisks), small intestine (second row), lymph node (third row; follicles marked with white asterisks), and spleen (fourth row; lymphoid regions enclosed by dashed circle). Images are hematoxylin and eosin with magnification indicated.

(d) Immunofluorescence microscopy of splenic sections with anti-B220 (green), anti-CD8 and anti-CD4 (red), and DAPI (blue).
(e) Analysis of splenocytes by flow cytometry shows severe B cell deficiency in *Adar*$^{-/-}$*Mavs*$^{-/-}$ mice.
Mice in (c) were 20 days old. Mice in (d) were 15 days old. Mice in (e) were 13 days old.

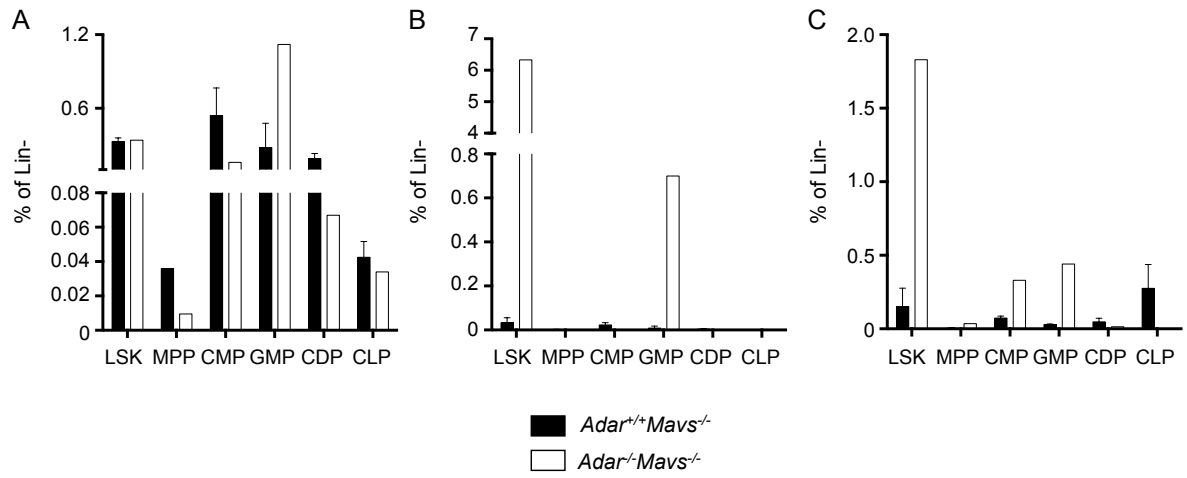

Figure 3.2: Hematopoiesis is mostly normal in Adar$^{-/-}$Mavs$^{-/-}$ *mice*

(a) Percent of each hematopoietic subset in total Lineage negative cells in the bone marrow.

(b) Percent of each hematopoietic subset in total Lineage negative cells in the blood.

(c) Percent of each hematopoietic subset in total Lineage negative cells in the spleen.

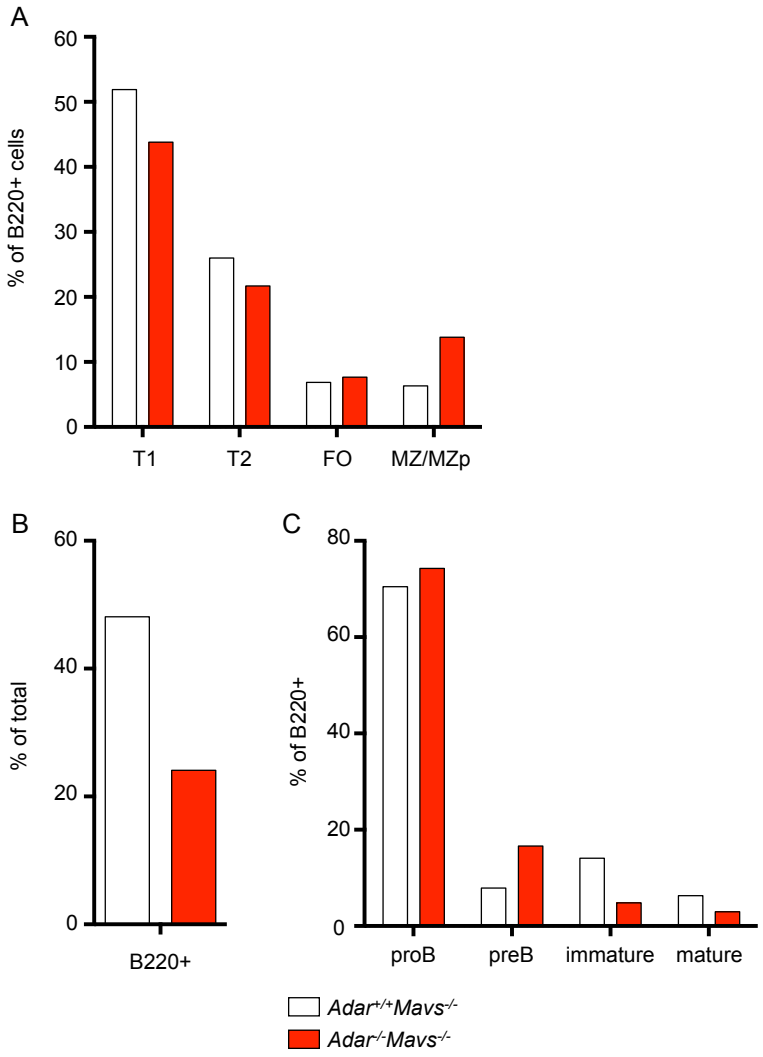

Figure 3.3: Adar$^{-/-}$Mavs$^{-/-}$ *mice have altered B cell development*

(**a)** Percent of B220+ splenic B cells of each of the noted developmental subsets

(b) Percent of B220+ B cells of total bone marrow cells.

(c) Percent of bone marrow B cells (B220+) of each of the noted developmental subsets.

Mice are 15 days old; n=1 of each.

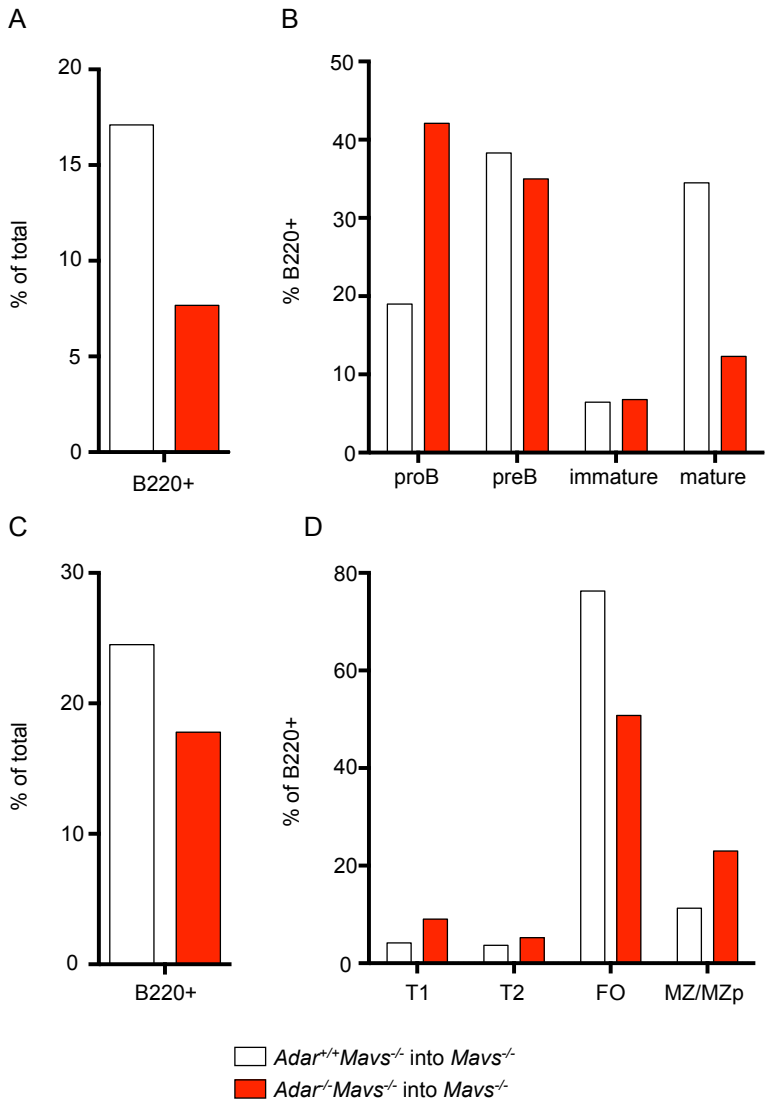

Figure 3.4: B cell deficiency is maintained in Adar$^{-/-}$Mavs$^{-/-}$ *bone marrow chimeras*

(a) Percent of B220+ B cells of total bone marrow cells.

(b) Percent of bone marrow B cells (B220+) of each of the noted developmental subsets.

(c) Percent of B220+ B cells in total splenocytes.

(**d**) Percent of B220+ splenic B cells of each of the noted developmental subsets

For both chimeras, n=1

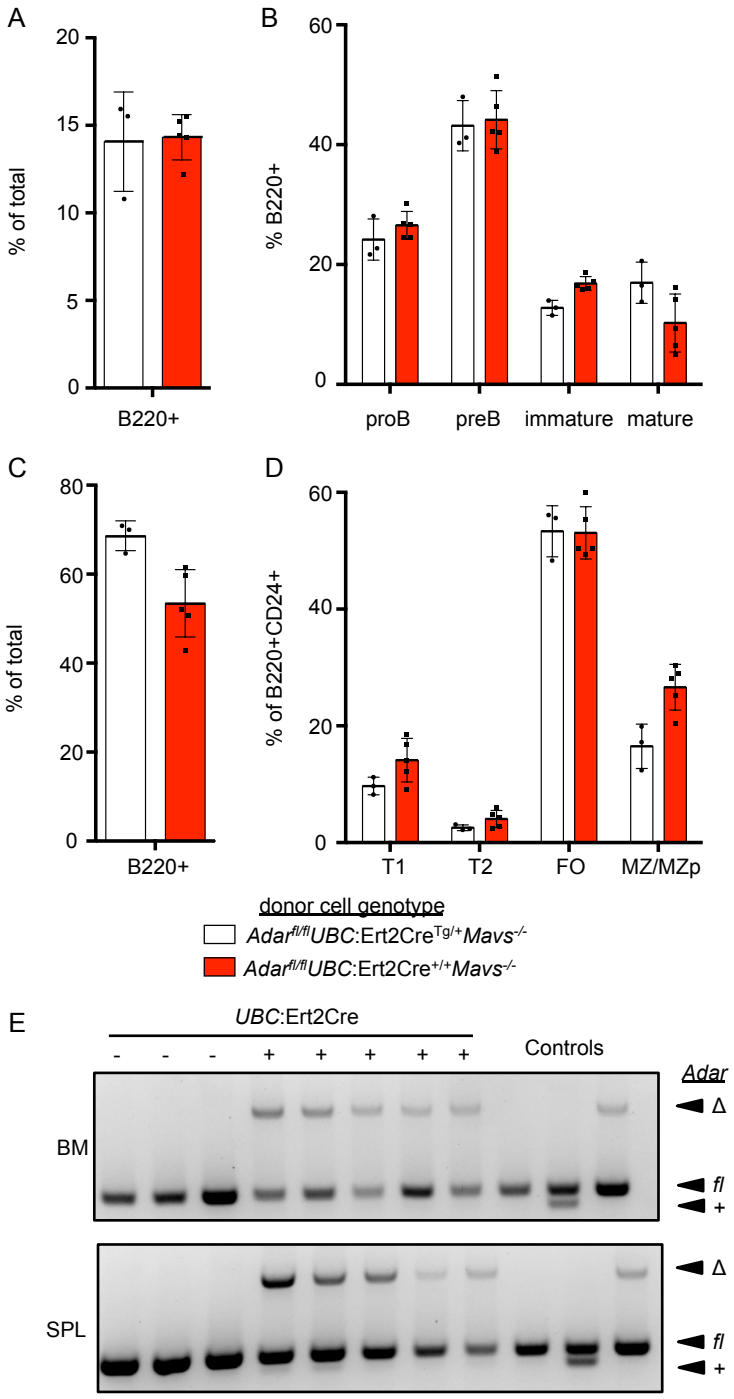

Figure 3.5: Inducible Adar*-deletion in bone marrow does not recapitulate* Adar$^{-/-}$Mavs$^{-/-}$ *bone marrow*

(a) Percent of B220+ B cells of total bone marrow cells.

(b) Percent of bone marrow B cells (B220+) of each of the noted developmental subsets.

(c) Percent of B220+ B cells in total splenocytes.

(**d)** Percent of B220+CD24+ splenic B cells of each of the noted developmental subsets

For *Adar*$^{fl/fl}$*UBC*:Ert2Cre$^{Tg/+}$*Mavs*$^{-/-}$ chimeras, n=3. For *Adar*$^{fl/fl}$*UBC*:Ert2Cre$^{+/+}$*Mavs*$^{-/-}$ chimeras, n=5.

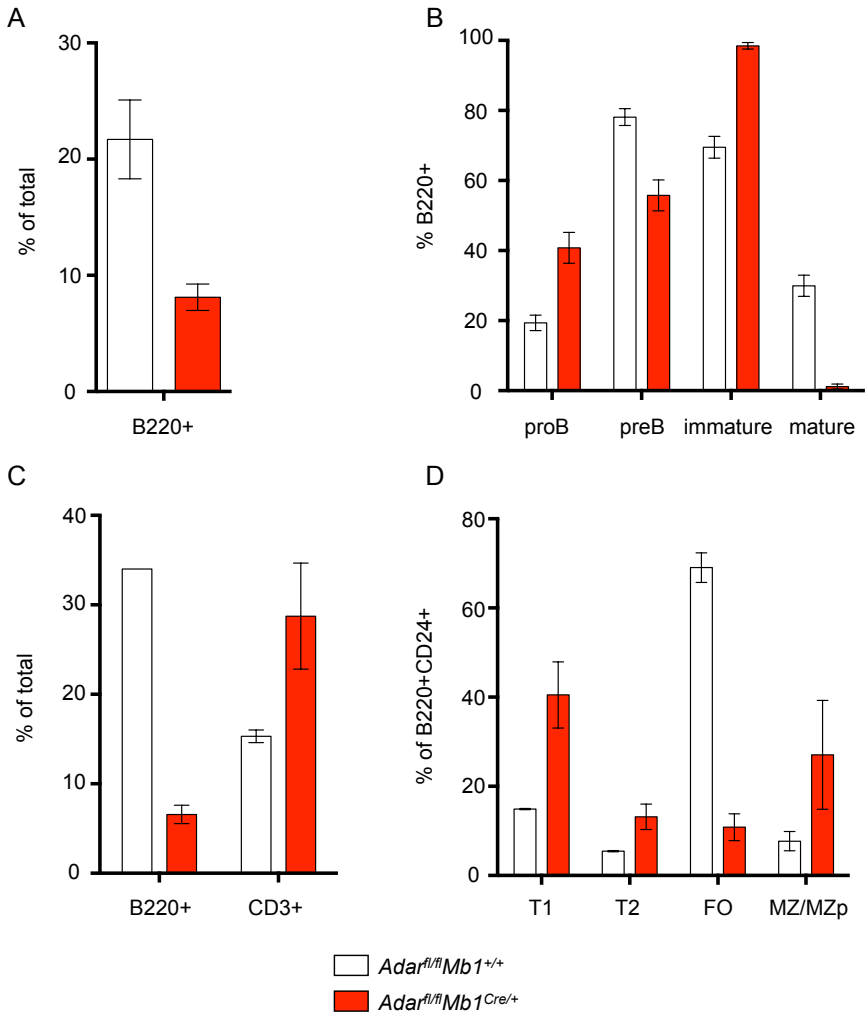

Figure 3.6: ADAR1-dependent B cell deficiency is cell intrinsic

(a) Percent of B220+ B cells of total bone marrow cells.

(b) Percent of bone marrow B cells (B220+) of each of the noted developmental subsets.

(c) Percent of B220+ B cells or CD3+ T cells in total splenocytes.

(d) Percent of B220+CD24+ splenic B cells of each of the noted developmental subsets

For *Adar*$^{fl/fl}$*Mbi*$^{+/+}$, n = 2. For *Adar*$^{fl/fl}$*Mb1*$^{Cre/+}$, n=3. Mice are 11-14 weeks old

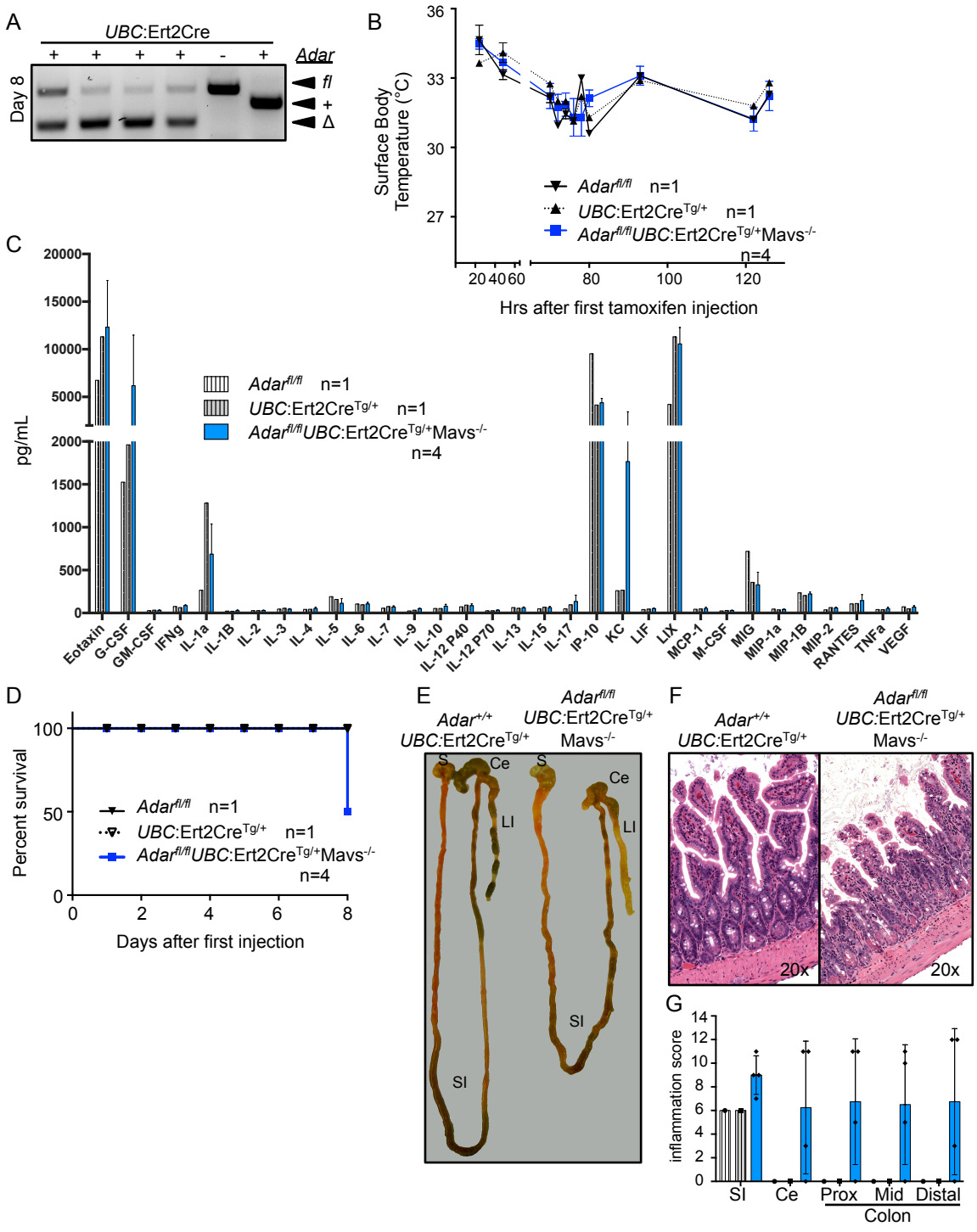

Figure 3.7: ADAR1 regulates tissue homeostasis in adults

(a) Samples of the ear were genotyped for *Adar* deletion after tamoxifen treatment.

(b) Surface body temperate readings for tamoxifen-treated mice at 20–120 hr after initial tamoxifen injection.

(c) Serum cytokine levels determined from mice at day 8.

(d) Surivial curve for mice treated with tamoxifen

(e) Ex vivo dissection of the gastrointestinal tract at day 8; stomach (S), small intestine (SI), cecum (Ce), and large intestine (LI) are indicated.

(f) Representative hematoxylin and eosin-stained ileum sections of tamoxifen-treated mice of the indicated genotypes at day 8. Original magnification is indicated in the bottom right.

(g) Histological scoring of inflammation in the gut at day 8. Abbreviations are as follows: SI, small intestine; CE, cecum; Prox, proximal colon; Mid, mid-colon.

Mean inflammation score of *Adar*$^{fl/fl}$*Mavs*$^{-/-}$*UBC:*Ert2Cre+ intestines compared to either control is significant by one-way ANOVA, p = 0.002

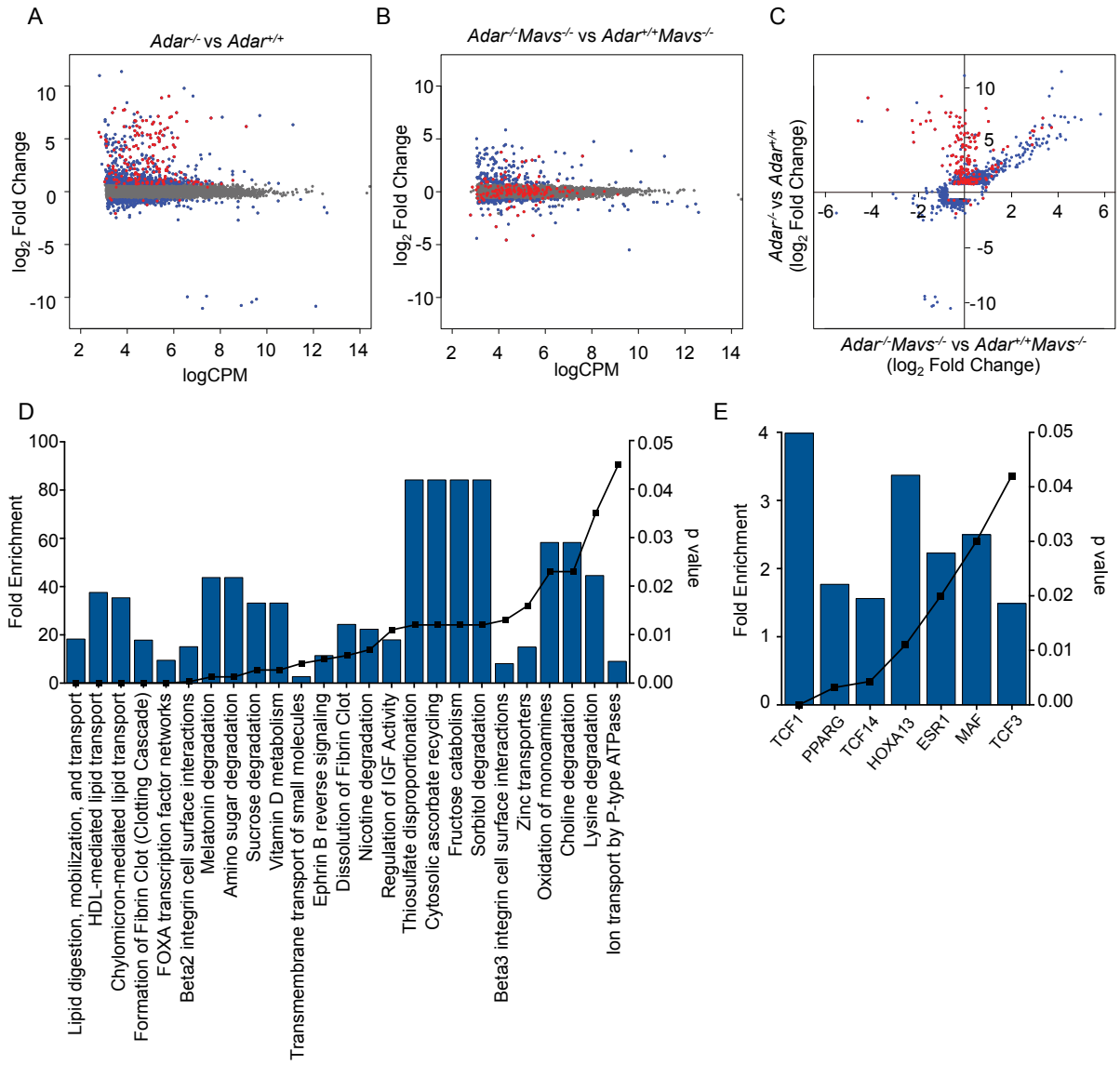

Figure 3.8: MAVS-Dependent and MAVS-Independent Gene Expression in Adar$^{-/-}$ *Embryos*

RNA-seq was performed on rRNA-depleted RNA from whole E11.5 embryos of the indicated genotypes.
(a) Comparison of gene expression between *Adar*$^{-/-}$ (n = 3) and *Adar*$^{+/+}$ (n = 3) embryos. Data are plotted as log2 fold change in gene expression on the y axis, with normalized log2 counts per million (CPM) on the x axis. Grey dots

denote genes with insignificant differences in expression. Blue dots denote non-ISGs with differential expression ($p < 0.01$). Red dots indicate ISGs with differential expression ($p < 0.01$).

(b) Comparison of gene expression between *Adar*$^{-/-}$*Mavs*$^{-/-}$ (n = 3) and *Mavs*$^{-/-}$ (n = 3) embryos, using the same criteria as in **(a)**.

(c) Genes with differential expression ($p < 0.01$) in either pairwise comparison were plotted, with *Adar*$^{-/-}$ versus *Adar*$^{+/+}$ on the y axis, and *Adar*$^{-/-}$*Mavs*$^{-/-}$ versus *Mavs*$^{-/-}$ on the x axis. Blue and red genes are the same as **(a)** and **(b)**.

(d) Biological pathways enriched among the genes with dysregulated expression in both Adar-/- embryos and *Adar*$^{-/-}$*Mavs*$^{-/-}$embryos identified in **(c)**.

(e) Transcription factor binding sites enriched in the MAVS-independent differentially expressed genes from **(c)**.

For **(d)** and **(e)**, fold enrichment relative to the representation of these pathways in the genome is shown on the left y axis and the blue bars. Significance of enrichment is indicated by hyper geometric p value on the right y axis and the black symbols/line. Analysis was performed with FunRich software

Chapter 4: Differential roles for the two isoforms of ADAR1

Introduction

In 1995, an interferon-inducible mammalian ADAR was discovered through a screen of cDNA clones of human interferon-regulated protein (47, 48). Over the next 10 years it was determined that this cDNA encodes for the p150 kDa isoform of ADAR1. The two isoforms of ADAR1 are produced from a single gene through alternative initiation sites and distinct promoters. Thus, two separate proteins are created from the same gene with different expression patterns, distinct protein domains, and, potentially, different functions. This is further supported by the fact that the unique promoter for the p150 isoform is interferon inducible, suggesting a role for ADAR1 p150 in antiviral immunity. (49-52)

Most papers that address the role of ADAR1 treat it as though it produces a single protein product, though a few papers have speculated that there may be individual roles for the ADAR1 isoforms. In 2011, the Oldstone lab at TSRI in San Diego generated a p150-specific knockout through homologous recombination of the unique exons of p150 with a Neo cassette. (53). They reported that the p150-specific knockout was embryonic lethal by day 12, which is consistent with what is observed in the complete *Adar* knockout that lacks both isoforms. Additionally, there are AGS-associated mutations that effect only the p150 isoform of ADAR1, and there are patients where the other allele is a null, suggesting that a dysfunctional p150 is enough to cause the interferonopathy. In a report by Mannion, et al, the AGS mutations in ADAR1 affected the ability of ADAR1 p150 to edit a known substrate more than they affected ADAR1 p110 (36).

As the embryonic lethality of the complete *Adar* knockout is fully rescued on MAVS-deficient background, we hypothesized that ADAR1 p150 alone may be the regulator of the MDA5/MAVS signaling pathway. After determining that the Adarp150-deficient mice were, in fact, deficient for just the p150 isoform (see Matthaei, Frese (54), Steinman and Wang (55)), we

crossed them to MAVS-deficient mice to generate double knockout mice. We find that ADAR1 p150 is the sole regulator of the MDA5/MAVS-pathway and also uncovered previously unknown distinct roles for p150 and p110 in cellular biological functions. These findings show that ADARs and RNA editing have critical roles in biology, but what role does ADAR1 play, specifically?

Results

We confirmed the absence of just p150 by Western blot (Fig 4.1a) before intercrossing *Adar p150*$^{+/-}$*Mavs*$^{-/-}$ mice. Like the *Adar*$^{-/-}$*Mavs*$^{-/-}$ mice, *Adar p150*$^{-/-}$*Mavs*$^{-/-}$ mice are recovered at normal Mendelian ratios (Fig. 4.1b) at birth. Unlike the *Adar*$^{-/-}$*Mavs*$^{-/-}$ mice, *Adar p150*$^{-/-}$ *Mavs*$^{-/-}$ mice are far healthier and have a vastly increased average lifespan of 18 days (Fig 4.1c). This is in stark contrast to the 95% of *Adar*$^{-/-}$*Mavs*$^{-/-}$ mice that die within two days. This shows that *Adar*-dependent embryonic lethality, which is due to autoinflammation downstream of aberrant MAVS-signaling, is completely dependent on ADAR1 p150.

The histological analysis of these mice revealed that the extremely disordered kidney we observed in the *Adar*$^{-/-}$*Mavs*$^{-/-}$ mice was restored to normalcy in the *Adar p150*$^{-/-}$*Mavs*$^{-/-}$ mice (Fig 4.2a). The intestines still show inflammation and the lymph nodes and spleen lacked B cell follicles (Fig 4.2b), which we confirmed by flow cytometry (Fig 4.2c). Furthermore, we amplified from the brain a region of the 5-HT2C receptor mRNA that is a known target of ADAR1 and sent it for Sanger sequencing. We confirmed that *Adar*$^{-/-}$*Mavs*$^{-/-}$ mice lack editing at the A and B sites in the 5-HT2CR transcript and that these are fully restored in an *Adar p150*$^{-/-}$*Mavs*$^{-/-}$ brain (Fig 4.2d). This data shows distinct biological roles for the individual ADAR1 isoforms. Furthermore, we can attribute specific events to individual isoforms.

Discussion

We now know that not only are there are duals roles for ADAR1 in innate immunity and cell biology, there are distinct roles for the two isoforms of ADAR1. ADAR1 truly is two separate enzymes and should not be treated as a single entity. We have shown that ADAR1 p150 is essential for negative regulation of the MDA5/MAVS pathway and has roles in regulating B cell development and maintenance of the gastrointestinal system. The extent of the role of p150 in the intestines is, again, complicated by the runted stature of the *Adar p150*$^{-/-}$*Mavs*$^{-/-}$ mice, which allows them to continue nursing well past 25 days of age. Thus, again, the *Adar p150*$^{-/-}$*Mavs*$^{-/-}$ mice we analyzed by histology had a different diet than their *Adar p150*$^{+/+}$*Mavs*$^{-/-}$ littermates, as mentioned previously for the *Adar*$^{-/-}$*Mavs*$^{-/-}$ mice. ADAR1 p110 contributes more to the developmental and physiological roles in maintaining normal bodily function, such as kidney structure and serotonin receptor expression.

While we have identified some differences in function between the two isoforms, there is still a lot we do not know. The differential roles of these isoforms could be further studied by comparing tissues and/or embryos from the *p150*$^{-/-}$*Mavs*$^{-/-}$ mice with those from the *Adar*$^{-/-}$*Mavs*$^{-/-}$ mice. The *ADARnull* 293T cells could be reconstituted with either or both isoform and differential editing and gene expression could be compared. Furthermore, the promoter and 5'UTR for ADAR1 p110 are upstream of those elements for ADAR1 p150. Thus, it would be possible to genetically modify those regions while leaving ADAR1 p150 intact. If this is successful, one could generate a mouse that lacks ADAR1 p110 while retaining expression of ADAR1 p150. If ADAR1 p150 is truly the exclusive negative regulator of MDA5/MAVS, this mouse would have no autoinflammation and would be born at normal Mendelian ratios like the *Adar*$^{-/-}$*Mavs*$^{-/-}$ mice, yet will still succumb to pathologies as a result of ADAR1 p110 deficiency including, potentially, issues with the brain and kidneys.

Chapter 4 Figures

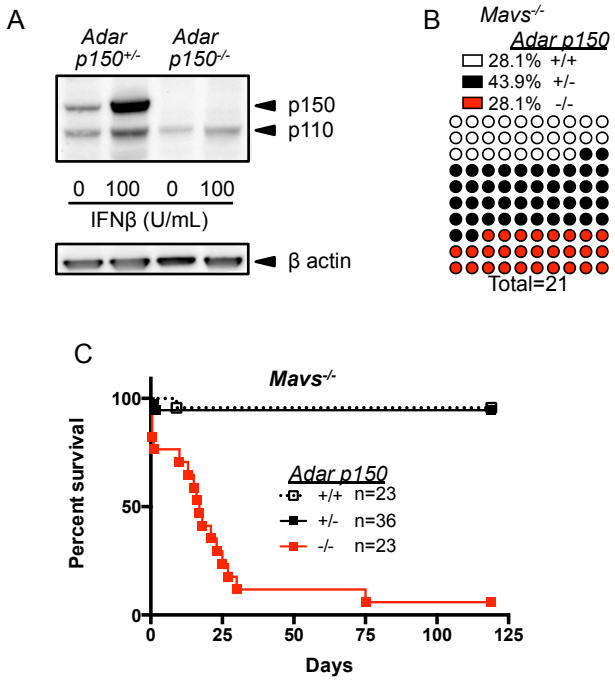

Figure 4.1: ADAR1 p150 is the negative regulator of MDA5-MAVS signaling pathway

(a) Immunoblot of ADAR1 protein expression in *p150*$^{+/-}$ or *p150*$^{-/-}$ MEFs

(b) Live births for mice from the *p150*$^{+/-}$*Mavs*$^{-/-}$ intercross

(c) Postnatal survival curves for mice from the *p150*$^{+/-}$*Mavs*$^{-/-}$ intercross

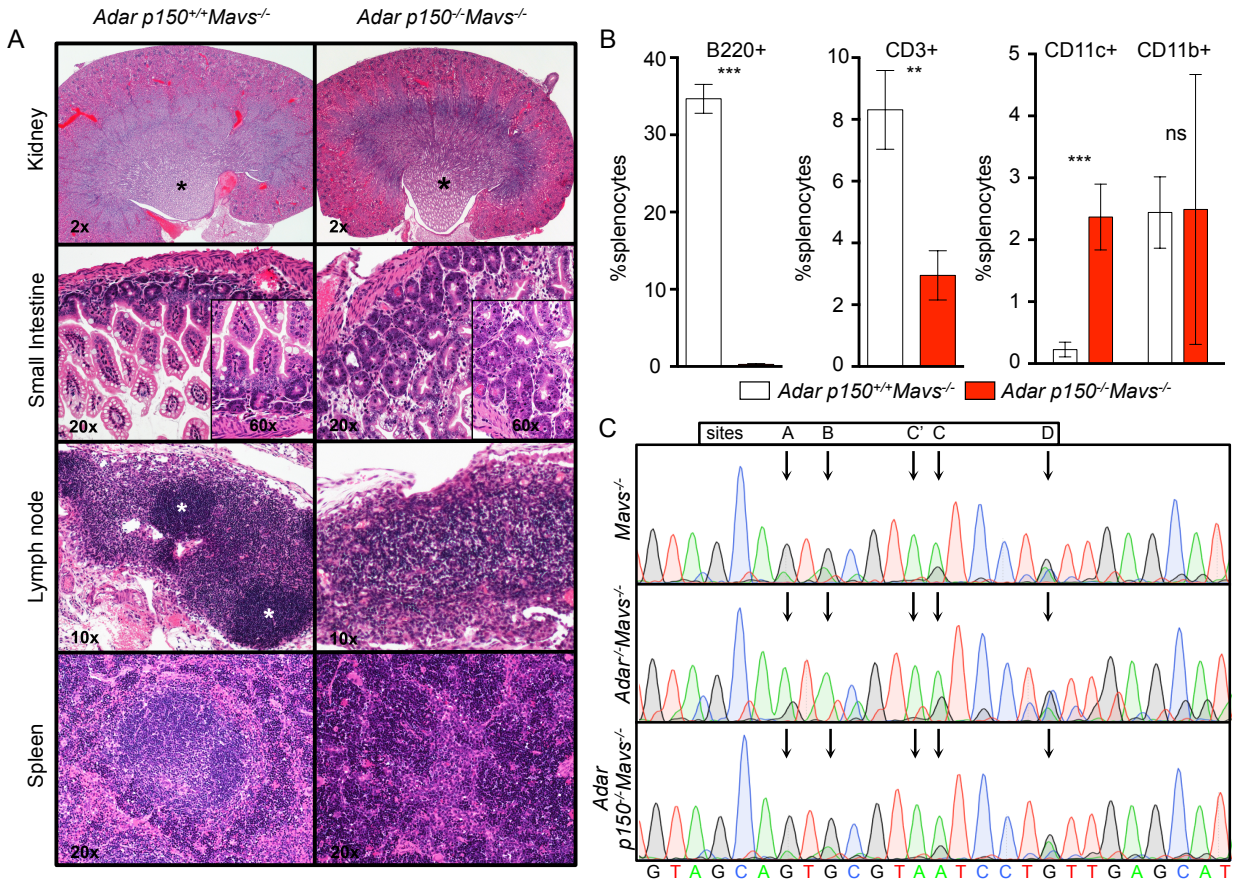

Figure 4.2: Distinct roles for the two isoforms of ADAR1 in development

(a) Hematoxylin and eosin-stained tissue sections of the indicated organs of *p150*$^{-/-}$*Mavs*$^{-/-}$ mice and controls are shown, with magnification indicated.

(b) Analysis of splenocytes by flow cytometry shows severe B cell deficiency and an increase in CD11c+ myeloid cells in *p150*$^{-/-}$*Mavs*$^{-/-}$ mice. Two-sample t test for p values; *p150*$^{+/+}$*Mavs*$^{-/-}$ n = 3, *p150*$^{-/-}$*Mavs*$^{-/-}$ n = 3; ***p < 0.002, **p = 0.004.

(c) Representative chromatograms of 2-HT2C receptor transcript editing in brains of 15- to 21-day-old mice of the indicated genotypes.

Mice in **(a)** were 15 days old. Mice in **(b)** and **(c)** were 21 days old.

Chapter 5: Materials and Methods

Mice and cells

Adar$^{fl/fl}$ mice were kindly provided by Dr. Stuart Orkin (Hartner et al., 2009) and were bred to B6.129S4-Meox2tm1(cre)Sor mice to delete the *Adar* allele in the germline, and to B6;129S-Tg(UBC-cre/ERT2)1Ejb to allow for tamoxifen-induced widespread deletion of Adar in adult mice. Both Cre-expressing mouse lines were purchased from the Jackson Laboratory (stock numbers 003755 and 008085). The *Adar*$^{+/-}$ mice resulting from the B6.129S4-Meox2tm1(cre)Sor cross were subsequently bred to *Tmem173*$^{-/-}$ (*Sting*$^{-/-}$) mice (7), *Mavs*$^{-/-}$ mice (14), *Ddx58*$^{-/-}$ (*Rigi*$^{-/-}$) mice (8), *Ifih1*$^{-/-}$ (*Mda5*$^{-/-}$) mice (56), *Ifnar1*$^{-/-}$ mice (Dr. Murali-Krishna Kaja), *Tnfr1*$^{-/-}$ (*Tnfrsf1a*^{tm1Mak}/J), or *Ripk3*$^{-/-}$ mice (57). *Ripk3*$^{-/-}$ mice were a gift to Oberst Lab from Kim Newton. *Adar p150*$^{+/-}$ gametes were generously provided by Dr. M. B. A. Oldstone (53). Sentinel mice (Crl:CD1[ICR]; Charles River, Wilmington, MA) were tested quarterly for endo- and ectoparasites, mouse hepatitis virus, mouse parvovirus, and rotavirus; and tested annually for Mycoplasma pulmonis, pneumonia virus of mice, reovirus 3, Sendai virus, and Theiler murine encephalomyelitis virus. All experiments were done in accordance with the Institutional Animal Care and Use Committee guidelines of the University of Washington.

Histology

Tissues were fixed in 10% neutral buffered formalin, paraffin embedded, cut into 4-5µm sections and routinely stained with hematoxylin and eosin. All tissues were coded to remove genotype identification. Tissues evaluated included lung, heart, esophagus, kidney, ureter, bladder, liver, pancreas, spleen, lymph nodes, salivary glands, stomach, small intestine, large intestine, and reproductive tract. Additionally, for the *Adar*$^{-/-}$*Mavs*$^{-/-}$ mice, decalcified cross sectional images of the skull and brain were also evaluated.

Flow cytometry and Cytokine Measurements

Single cell suspensions from spleen, bone marrow, thymus or blood were isolated and stained with antibodies for CD3 (145-2C11), CD4 (RM4-5), CD8β (H35-17.2), B220 (RA3-6B2), CD11c (N418), CD11b (M1/70), CD45.2 (104), and/or Ter119; Cells were analyzed with a FACSCanto (BD Biosciences) and analyzed with FlowJo software (TreeStar). Measurement of serum cytokines was performed using the Milliplex-70K-PX32 mouse cytokine/chemokine magnetic bead panel (Millipore), according to the manufacturers instructions.

Immunofluorescence microscopy

Spleens were frozen in Optimal Cutting Temperature (OCT) media (Sakura). Tissues were cut into 7-µm sections and treated with ice-cold acetone. Sections were stained with directly conjugated antibodies: CD8α (53-6.7, eBioscience), CD4 (RM4-5, eBioscience), and B220 (RA3-6B2, eBioscience). Nuclei were stained with 1 ug/mL DAPI. Stained slides were mounted with Prolong Gold antifade reagent (Life Technologies), imaged using a Nikon Eclipse 90i microscope and analyzed using Adobe Photoshop software.

Quantitative RT-PCR

Embryos were harvested into TRIzol (Life Technologies), homogenized through an 18-G needle attached to a 3 mL syringe, followed by RNA extraction according to manufacturer's instructions. RNA was treated with DNase (Ambion) and 1 µg was reverse-transcribed using RNA to cDNA EcoDry™ Premix (Double Primed) (Clontech). cDNA was used for PCR with EVA Green reagents (Bio-Rad Laboratories) on a Bio-Rad CFX96 Real-Time System. The abundance of each interferon-stimulated gene mRNA was normalized to that of HPRT mRNA and results were compared with genetic control embryos for calculation of relative induction.

The primers used were:

Cxcl10 Fwd:AAGTGCTGCCGTCATTTTCTGCCTC, Cxcl10 Rev:CTTGATGGTCTTAGATTCCGGATTC;

Isg15 Fwd:GGTGTCCGTGACTAACTCCAT, Isg15 Rev:TGGAAAGGGTAAGACCGTCCT;

Ifit1 Fwd:GCCATTCAACTGTCTCCTG, Ifit1 Rev:GCTCTGTCTGTGTCATATACC;

Ifit2 Fwd:AGTACAACGAGTAAGGAGTCACT, Ifit2 Rev:AGGCCAGTATGTTGCACATGG (Primer bank ID: 6680363a1);

Mx1 Fwd:GACCATAGGGGTCTTGACCAA, Mx1 Rev:AGACTTGCTCTTTCTGAAAAGCC (Primer bank ID: 6996930a1);

Rsad2 Fwd:TGCTGGCTGAGAATAGCATTAGG, Rsad2 Rev:GCTGAGTGCTGTTCCCATCT (Primer bank ID: 31543946a1);

Hprt Fwd:GTTGGATACAGGCCAGACTTTGTTG, Hprt Rev:GAGGGTAGGCTGGCCTATAGGCT (Spandidos et al., 2010);

Htr2c (5ht2c) Fwd:TGTCCCTAGCCATTGCTGATATG, Htr2c Rev:TGTCAACGGGATGAAGAATGCC.

Deletion of ADAR1 in adult mice

Tamoxifen-induced deletion was performed according to the protocol available from the Jackson Laboratory. In brief, tamoxifen (Sigma-Aldrich) was dissolved in corn oil (Sigma-Aldrich) at 20 mg/mL overnight at 37°C, filtered through a 0.22 μm Millex GP PES membrane and stored at 4°C. Mice were administered 100 μL of tamoxifen via i.p. injection once a day for three days. On day four, *Adar*$^{fl/fl}$*Mavs*$^{+/+}$ Cre-positive mice were moribund, so no further injections were given. Mice were sacrificed and analyzed by histology and flow cytometry.

RNA-Seq library preparation

Total RNA was harvest from embryos as described above. Ribosomal RNA was depleted using the RiboZero™ Magnetic Kit (Human/Mouse/Rat) from Illumina. Libraries were prepared from the Ribo-depleted RNA using the NEBNext® Ultra™ RNA Library Prep Kit for Illumina® (New England BioLabs) with the following modifications: Ribo-depleted RNA was fragmented for 5 min at 94°C to obtain >300bp fragments and first strand synthesis reaction was incubated for 50 min at 42°C. PCR Library enrichment was performed using the KAPA HiFi DNA Polymerase (KAPA Biosystems) with Illumina barcoded sequencing primers. Library size distribution was confirmed on an Agilent 2100 Bioanalyzer with a High Sensitivity DNA Chip (Agilent Technologies). Barcoded libraries were combined and sequenced with an Illumina NextSeq, resulting in approximately 60 million paired-end 150-base pair sequencing reads per embryo.

Alignment and analysis of RNA-Seq data

Fastq files were aligned using STAR 2.4.2a (58), with the following parameters for the indices: STAR --runMode genomeGenerate --genomeDir /m}t/indices/ --genomeFastaFiles /mnt/genome/Mus_musculus.GRCm38.dna.SORTED.fa--sjdbGTFfile /mnt/transcriptome/Mus_musculus.GRCm38.81.gtf --runThreadN 32 .

Alignment was performed with the following parameters: STAR --genomeDir /mnt/indices/ --readFilesIn /mnt2/data/run2/${i}_R1.fastq.gz /mnt2/data/run2/${i}_R2.fastq.gz --readFilesCommand zcat --runThreadN 32 --outSAMtype BAM SortedByCoordinate --quantMode GeneCounts --outFilterMismatchNmax 30 --outFileNamePrefix /mnt/results/run2/${i}.star. --outFilterMultimapNmax 20 --outSAMattributes All .

All alignments were performed on Amazon EC2 c3.8xlarge instance using a Ubuntu13.04 base AMI. The read count files produced by STAR (unstranded) were used for differential expression analysis using the Bioconductor package edgeR (59). Following calculation of the normalization factors, low-expressing genes were discarded. Counts were then subject to the estimateGLMCommonDisp function followed by glmFit. Differential expression for comparison between phenotypes was then performed using the glmLRT function. ISGs were annotated using the Interferome web tool (http://www.interferome.org/interferome/search/showSearch.jspx), defined as all Type I IFN-regulated genes in all tissues of Mus musculus with a cutoff of 3-fold expression. Read count and fastq files are available at SRA. For bioinformatics analysis, we used FunRich software (60) to determine the enrichment of specific biological pathways and transcription factor networks among genes with dysregulated expression in both *Adar*$^{-/-}$ and *Adar*$^{-/-}$*Mavs*$^{-/-}$ embryos, relative to the representation of these pathways in the genome.

CRISPR targeting of ADAR1 in human cells

For targeting of ADAR with CRISPR-Cas9, we used a lentiviral vector in which an RNA polymerase III promoter–driven guide RNA and an RNA polymerase II promoter–driven Cas9-T2A cassette (including sequence encoding a protein for resistance to puromycin) were constitutively expressed from a single, self-inactivating lentivirus upon integration into the host cell genome. Lentivirus pseudotyped with vesicular stomatitis virus envelope glycoprotein was produced by transfection of 2.5 × 106 HEK 293T cells for 48 h in 10-cm plates with 10 μg of the CRISPR-Cas9 ADAR targeting construct, 9 μg psPAX-2 (a lentiviral packaging plasmid) and 1 μg pVSV-G (plasmid encoding vesicular stomatitis virus envelope glycoprotein). 2.5 × 10^6 HEK 293T cells were transduced with the viral supernatants on day 3 after harvest, then were selected for 3 d with 5 μg/ml puromycin (Life Technologies). Subsequent single-cell cloning was performed by serial dilution. Targeting of the ADAR locus via CRISPR was evaluated by

restriction fragment length polymorphism with an ApoI (New England Biolabs) restriction site that overlapped the CRISPR targeting site. Products were separated by electrophoresis through a 3% MetaPhor agarose gel (Lonza). ADAR mutations were identified by PCR amplification of the surrounding sequence, cloning into pCDNA3, and sequencing of nine independent plasmids. ADAR1 protein loss was confirmed by immunoblot analysis of whole-cell extracts with or without 24 hours of human IFNβ treatment (100 U/mL, R&D Systems) with rabbit polyclonal anti-ADAR1 (12317; Cell Signaling Technologies) and mouse monoclonal anti-β actin (AC-74; Sigma). The guide RNA target sequence is (sense), 5′ -GGACAGGAGACGGAATTCGC-**3′ .**

ISRE-luciferase reporter assays

1×10^5 HEK 293T cells with or without ADAR1 expression in 24 well plates were transfected with 25 ng ISRE-luciferase reporter plasmid (Takara Bio Inc.) with 0, 12.5, 25, 50, 100, or 200 ng of pCDNA3.1-expressing human RLRs using Lipofectamine® 2000 (Life Technologies) and then incubated for 24 h. Cells were lysed in Passive Lysis Buffer (Promega) and luciferase activity was assessed using the Luciferase Reporter Assay System (Promega) according to the manufacturer's instructions and read using a Centro LB 960 Luminometer (Berthold Technologies).

Statistical Analysis

Statistical significance of difference between groups was assessed using Wilcoxon Rank Sum, Chi Square Goodness-of-fit or two-way ANOVA with Tukey's multiple comparison test, as indicated in the figure legends. Values of $p<0.05$ were considered statistically significant. All analyses were performed using Prism v6.0 software (GraphPad).

References

1. Janeway CA, Jr. Approaching the asymptote? Evolution and revolution in immunology. Cold Spring Harbor symposia on quantitative biology. 1989;54 Pt 1:1-13. PubMed PMID: 2700931.
2. Medzhitov R. Approaching the asymptote: 20 years later. Immunity. 2009 Jun 19;30(6):766-75. PubMed PMID: 19538928.
3. Szentivanyi A, Friedman H. The Immunologic revolution : facts and witnesses. Boca Raton: CRC Press; 1994. 419 p. p.
4. tenOever BR. The Evolution of Antiviral Defense Systems. Cell host & microbe. 2016 Feb 10;19(2):142-9. PubMed PMID: 26867173.
5. Barbalat R, Ewald SE, Mouchess ML, Barton GM. Nucleic acid recognition by the innate immune system. Annu Rev Immunol. 2011 Apr 23;29:185-214. PubMed PMID: 21219183. Epub 2011/01/12. eng.
6. Sun L, Wu J, Du F, Chen X, Chen ZJ. Cyclic GMP-AMP synthase is a cytosolic DNA sensor that activates the type I interferon pathway. Science. 2013 Feb 15;339(6121):786-91. PubMed PMID: 23258413. Pubmed Central PMCID: 3863629.
7. Ishikawa H, Barber GN. STING is an endoplasmic reticulum adaptor that facilitates innate immune signalling. Nature. 2008 Oct 2;455(7213):674-8. PubMed PMID: 18724357. Pubmed Central PMCID: 2804933. Epub 2008/08/30. eng.
8. Kato H, Sato S, Yoneyama M, Yamamoto M, Uematsu S, Matsui K, et al. Cell type-specific involvement of RIG-I in antiviral response. Immunity. 2005 Jul;23(1):19-28. PubMed PMID: 16039576.
9. Kato H, Takeuchi O, Sato S, Yoneyama M, Yamamoto M, Matsui K, et al. Differential roles of MDA5 and RIG-I helicases in the recognition of RNA viruses. Nature. 2006 May 4;441(7089):101-5. PubMed PMID: 16625202.
10. Seth RB, Sun L, Ea CK, Chen ZJ. Identification and characterization of MAVS, a mitochondrial antiviral signaling protein that activates NF-kappaB and IRF 3. Cell. 2005 Sep 9;122(5):669-82. PubMed PMID: 16125763.
11. Wu J, Chen ZJ. Innate immune sensing and signaling of cytosolic nucleic acids. Annu Rev Immunol. 2014;32:461-88. PubMed PMID: 24655297.
12. Schlee M, Hartmann G. Discriminating self from non-self in nucleic acid sensing. Nature reviews Immunology. 2016 Sep;16(9):566-80. PubMed PMID: 27455396.

13. Stetson DB, Ko JS, Heidmann T, Medzhitov R. Trex1 prevents cell-intrinsic initiation of autoimmunity. Cell. 2008 Aug 22;134(4):587-98. PubMed PMID: 18724932.
14. Gall A, Treuting P, Elkon KB, Loo YM, Gale M, Jr., Barber GN, et al. Autoimmunity Initiates in Nonhematopoietic Cells and Progresses via Lymphocytes in an Interferon-Dependent Autoimmune Disease. Immunity. 2012 Jan 27;36(1):120-31. PubMed PMID: 22284419. Pubmed Central PMCID: 3269499. Epub 2012/01/31. eng.
15. Crow YJ, Hayward BE, Parmar R, Robins P, Leitch A, Ali M, et al. Mutations in the gene encoding the 3'-5' DNA exonuclease TREX1 cause Aicardi-Goutieres syndrome at the AGS1 locus. Nat Genet. 2006 Aug;38(8):917-20. PubMed PMID: 16845398.
16. Crow YJ, Leitch A, Hayward BE, Garner A, Parmar R, Griffith E, et al. Mutations in genes encoding ribonuclease H2 subunits cause Aicardi-Goutieres syndrome and mimic congenital viral brain infection. Nat Genet. 2006 Aug;38(8):910-6. PubMed PMID: 16845400.
17. Rice GI, Bond J, Asipu A, Brunette RL, Manfield IW, Carr IM, et al. Mutations involved in Aicardi-Goutieres syndrome implicate SAMHD1 as regulator of the innate immune response. Nat Genet. 2009 Jul;41(7):829-32. PubMed PMID: 19525956. Epub 2009/06/16. eng.
18. Rice GI, Kasher PR, Forte GM, Mannion NM, Greenwood SM, Szynkiewicz M, et al. Mutations in ADAR1 cause Aicardi-Goutieres syndrome associated with a type I interferon signature. Nat Genet. 2012 Nov;44(11):1243-8. PubMed PMID: 23001123. Epub 2012/09/25. eng.
19. Rice GI, del Toro Duany Y, Jenkinson EM, Forte GM, Anderson BH, Ariaudo G, et al. Gain-of-function mutations in IFIH1 cause a spectrum of human disease phenotypes associated with upregulated type I interferon signaling. Nat Genet. 2014 May;46(5):503-9. PubMed PMID: 24686847. Pubmed Central PMCID: 4004585. Epub 2014/04/02. eng.
20. Aicardi J, Goutieres F. A progressive familial encephalopathy in infancy with calcifications of the basal ganglia and chronic cerebrospinal fluid lymphocytosis. Annals of neurology. 1984 Jan;15(1):49-54. PubMed PMID: 6712192.
21. Crow YJ, Chase DS, Lowenstein Schmidt J, Szynkiewicz M, Forte GM, Gornall HL, et al. Characterization of human disease phenotypes associated with mutations in TREX1, RNASEH2A, RNASEH2B, RNASEH2C, SAMHD1, ADAR, and IFIH1. American journal of medical genetics Part A. 2015 Feb;167A(2):296-312. PubMed PMID: 25604658. Pubmed Central PMCID: 4382202.

22. Lebon P, Badoual J, Ponsot G, Goutieres F, Hemeury-Cukier F, Aicardi J. Intrathecal synthesis of interferon-alpha in infants with progressive familial encephalopathy. J Neurol Sci. 1988 Apr;84(2-3):201-8. PubMed PMID: 2837539.
23. Rice GI, Forte GM, Szynkiewicz M, Chase DS, Aeby A, Abdel-Hamid MS, et al. Assessment of interferon-related biomarkers in Aicardi-Goutieres syndrome associated with mutations in TREX1, RNASEH2A, RNASEH2B, RNASEH2C, SAMHD1, and ADAR: a case-control study. Lancet neurology. 2013 Dec;12(12):1159-69. PubMed PMID: 24183309. Epub 2013/11/05. eng.
24. Gott JM, Emeson RB. Functions and mechanisms of RNA editing. Annual review of genetics. 2000;34:499-531. PubMed PMID: 11092837.
25. Novoa EM, Pavon-Eternod M, Pan T, Ribas de Pouplana L. A role for tRNA modifications in genome structure and codon usage. Cell. 2012 Mar 30;149(1):202-13. PubMed PMID: 22464330.
26. Gerber AP, Keller W. RNA editing by base deamination: more enzymes, more targets, new mysteries. Trends in biochemical sciences. 2001 Jun;26(6):376-84. PubMed PMID: 11406411.
27. Bass BL. RNA editing by adenosine deaminases that act on RNA. Annual review of biochemistry. 2002;71:817-46. PubMed PMID: 12045112. Pubmed Central PMCID: 1823043. Epub 2002/06/05. eng.
28. Yang W, Chendrimada TP, Wang Q, Higuchi M, Seeburg PH, Shiekhattar R, et al. Modulation of microRNA processing and expression through RNA editing by ADAR deaminases. Nature structural & molecular biology. 2006 Jan;13(1):13-21. PubMed PMID: 16369484. Pubmed Central PMCID: 2950615. Epub 2005/12/22. eng.
29. Savva YA, Rieder LE, Reenan RA. The ADAR protein family. Genome biology. 2012;13(12):252. PubMed PMID: 23273215. Pubmed Central PMCID: 3580408.
30. Schwartz T, Rould MA, Lowenhaupt K, Herbert A, Rich A. Crystal structure of the Zalpha domain of the human editing enzyme ADAR1 bound to left-handed Z-DNA. Science. 1999 Jun 11;284(5421):1841-5. PubMed PMID: 10364558. Epub 1999/06/12. eng.
31. Hartner JC, Schmittwolf C, Kispert A, Muller AM, Higuchi M, Seeburg PH. Liver disintegration in the mouse embryo caused by deficiency in the RNA-editing enzyme ADAR1. The Journal of biological chemistry. 2004 Feb 6;279(6):4894-902. PubMed PMID: 14615479. Epub 2003/11/15. eng.
32. Hartner JC, Walkley CR, Lu J, Orkin SH. ADAR1 is essential for the maintenance of hematopoiesis and suppression of interferon signaling. Nature immunology. 2009

Jan;10(1):109-15. PubMed PMID: 19060901. Pubmed Central PMCID: 2701568. Epub 2008/12/09. eng.

33. Bass BL, Weintraub H. An unwinding activity that covalently modifies its double-stranded RNA substrate. Cell. 1988 Dec 23;55(6):1089-98. PubMed PMID: 3203381.

34. Pestal K, Funk Cory C, Snyder Jessica M, Price Nathan D, Treuting Piper M, Stetson Daniel B. Isoforms of RNA-Editing Enzyme ADAR1 Independently Control Nucleic Acid Sensor MDA5-Driven Autoimmunity and Multi-organ Development. Immunity.43(5):933-44.

35. Wang Q, Khillan J, Gadue P, Nishikura K. Requirement of the RNA editing deaminase ADAR1 gene for embryonic erythropoiesis. Science. 2000 Dec 1;290(5497):1765-8. PubMed PMID: 11099415. Epub 2000/12/02. eng.

36. Mannion NM, Greenwood SM, Young R, Cox S, Brindle J, Read D, et al. The RNA-Editing Enzyme ADAR1 Controls Innate Immune Responses to RNA. Cell reports. 2014 Nov 20;9(4):1482-94. PubMed PMID: 25456137.

37. Bass BL, Weintraub H. A developmentally regulated activity that unwinds RNA duplexes. Cell. 1987 Feb 27;48(4):607-13. PubMed PMID: 2434241.

38. Chen SH, Habib G, Yang CY, Gu ZW, Lee BR, Weng SA, et al. Apolipoprotein B-48 is the product of a messenger RNA with an organ-specific in-frame stop codon. Science. 1987 Oct 16;238(4825):363-6. PubMed PMID: 3659919.

39. Powell LM, Wallis SC, Pease RJ, Edwards YH, Knott TJ, Scott J. A novel form of tissue-specific RNA processing produces apolipoprotein-B48 in intestine. Cell. 1987 Sep 11;50(6):831-40. PubMed PMID: 3621347.

40. Sommer B, Kohler M, Sprengel R, Seeburg PH. RNA editing in brain controls a determinant of ion flow in glutamate-gated channels. Cell. 1991 Oct 4;67(1):11-9. PubMed PMID: 1717158. Epub 1991/10/04. eng.

41. Feldmeyer D, Kask K, Brusa R, Kornau HC, Kolhekar R, Rozov A, et al. Neurological dysfunctions in mice expressing different levels of the Q/R site-unedited AMPAR subunit GluR-B. Nature neuroscience. 1999 Jan;2(1):57-64. PubMed PMID: 10195181.

42. Brusa R, Zimmermann F, Koh DS, Feldmeyer D, Gass P, Seeburg PH, et al. Early-onset epilepsy and postnatal lethality associated with an editing-deficient GluR-B allele in mice. Science. 1995 Dec 8;270(5242):1677-80. PubMed PMID: 7502080.

43. Higuchi M, Maas S, Single FN, Hartner J, Rozov A, Burnashev N, et al. Point mutation in an AMPA receptor gene rescues lethality in mice deficient in the RNA-editing enzyme ADAR2. Nature. 2000 Jul 6;406(6791):78-81. PubMed PMID: 10894545.

44. Jepson JE, Reenan RA. Adenosine-to-inosine genetic recoding is required in the adult stage nervous system for coordinated behavior in Drosophila. The Journal of biological chemistry. 2009 Nov 6;284(45):31391-400. PubMed PMID: 19759011. Pubmed Central PMCID: 2781535.

45. Tonkin LA, Saccomanno L, Morse DP, Brodigan T, Krause M, Bass BL. RNA editing by ADARs is important for normal behavior in Caenorhabditis elegans. The EMBO journal. 2002 Nov 15;21(22):6025-35. PubMed PMID: 12426375. Pubmed Central PMCID: 137199.

46. Sebastiani P, Montano M, Puca A, Solovieff N, Kojima T, Wang MC, et al. RNA editing genes associated with extreme old age in humans and with lifespan in C. elegans. PloS one. 2009;4(12):e8210. PubMed PMID: 20011587. Pubmed Central PMCID: 2788130.

47. Patterson JB, Samuel CE. Expression and regulation by interferon of a double-stranded-RNA-specific adenosine deaminase from human cells: evidence for two forms of the deaminase. Molecular and cellular biology. 1995 Oct;15(10):5376-88. PubMed PMID: 7565688. Pubmed Central PMCID: 230787.

48. Patterson JB, Thomis DC, Hans SL, Samuel CE. Mechanism of interferon action: double-stranded RNA-specific adenosine deaminase from human cells is inducible by alpha and gamma interferons. Virology. 1995 Jul 10;210(2):508-11. PubMed PMID: 7618288.

49. George CX, Das S, Samuel CE. Organization of the mouse RNA-specific adenosine deaminase Adar1 gene 5'-region and demonstration of STAT1-independent, STAT2-dependent transcriptional activation by interferon. Virology. 2008 Oct 25;380(2):338-43. PubMed PMID: 18774582. Pubmed Central PMCID: 2628478.

50. George CX, Samuel CE. Human RNA-specific adenosine deaminase ADAR1 transcripts possess alternative exon 1 structures that initiate from different promoters, one constitutively active and the other interferon inducible. Proceedings of the National Academy of Sciences of the United States of America. 1999 Apr 13;96(8):4621-6. PubMed PMID: 10200312. Pubmed Central PMCID: 16382.

51. George CX, Samuel CE. Characterization of the 5'-flanking region of the human RNA-specific adenosine deaminase ADAR1 gene and identification of an interferon-inducible ADAR1 promoter. Gene. 1999 Mar 18;229(1-2):203-13. PubMed PMID: 10095120.

52. George CX, Wagner MV, Samuel CE. Expression of interferon-inducible RNA adenosine deaminase ADAR1 during pathogen infection and mouse embryo development involves tissue-selective promoter utilization and alternative splicing. The Journal of biological chemistry. 2005 Apr 15;280(15):15020-8. PubMed PMID: 15677478.

53. Ward SV, George CX, Welch MJ, Liou LY, Hahm B, Lewicki H, et al. RNA editing enzyme adenosine deaminase is a restriction factor for controlling measles virus replication that also is required for embryogenesis. Proceedings of the National Academy of Sciences of the United States of America. 2011 Jan 4;108(1):331-6. PubMed PMID: 21173229. Pubmed Central PMCID: 3017198. Epub 2010/12/22. eng.

54. Matthaei KI, Frese M, Hill CE. Is the p150 isoform of the RNA editing enzyme Adenosine Deaminase 1 really responsible for embryonic lethality? Proceedings of the National Academy of Sciences of the United States of America. 2011 Mar 22;108(12):E43; author reply E4. PubMed PMID: 21402945. Pubmed Central PMCID: 3064400. Epub 2011/03/16. eng.

55. Steinman RA, Wang Q. ADAR1 isoform involvement in embryonic lethality. Proceedings of the National Academy of Sciences of the United States of America. 2011 Jun 14;108(24):E199; author reply E200. PubMed PMID: 21593418. Pubmed Central PMCID: 3116395.

56. Gitlin L, Barchet W, Gilfillan S, Cella M, Beutler B, Flavell RA, et al. Essential role of mda-5 in type I IFN responses to polyriboinosinic:polyribocytidylic acid and encephalomyocarditis picornavirus. Proceedings of the National Academy of Sciences of the United States of America. 2006 May 30;103(22):8459-64. PubMed PMID: 16714379. Pubmed Central PMCID: 1464000.

57. Newton K, Sun X, Dixit VM. Kinase RIP3 is dispensable for normal NF-kappa Bs, signaling by the B-cell and T-cell receptors, tumor necrosis factor receptor 1, and Toll-like receptors 2 and 4. Molecular and cellular biology. 2004 Feb;24(4):1464-9. PubMed PMID: 14749364. Pubmed Central PMCID: 344190.

58. Dobin A, Davis CA, Schlesinger F, Drenkow J, Zaleski C, Jha S, et al. STAR: ultrafast universal RNA-seq aligner. Bioinformatics. 2013 Jan 1;29(1):15-21. PubMed PMID: 23104886. Pubmed Central PMCID: 3530905.

59. Robinson MD, McCarthy DJ, Smyth GK. edgeR: a Bioconductor package for differential expression analysis of digital gene expression data. Bioinformatics. 2010 Jan 1;26(1):139-40. PubMed PMID: 19910308. Pubmed Central PMCID: 2796818.

60. Pathan M, Keerthikumar S, Ang CS, Gangoda L, Quek CY, Williamson NA, et al. FunRich: An open access standalone functional enrichment and interaction network analysis tool. Proteomics. 2015 Aug;15(15):2597-601. PubMed PMID: 25921073.